Supplementary Materials for

Mutations in the *neverland* gene turned *Drosophila pachea* into an obligate specialist species

Michael Lang, Sophie Murat, Andrew G. Clark, Géraldine Gouppil, Catherine Blais, Luciano M. Matzkin, Émilie Guittard, Takuji Yoshiyama-Yanagawa, Hiroshi Kataoka, Ryusuke Niwa, René Lafont, Chantal Dauphin-Villemant and Virginie Orgogozo

This file includes:

Materials and methods

Drosophila strains and fly culture

The *2-286-GAL4* (from C. S. Thummel) (*18*) and *UAS-nvd-RNAi-IR-1* (*8*) lines were described previously. Line w^{1118} was used for in situ hybridization. Non-*melanogaster* *Drosophila* species were obtained from the San Diego Drosophila Stock Center (San Diego, CA, USA): *D. pachea* (15090-1698.01, -1698.02 and -1698.05), *D. acanthoptera* (15090-1693.00), *D. nannoptera* (15090-1692.01), *D. wassermani* (15090-11697.11), *D. robusta* (15020-1111.10) and *D. mojavensis* (15081-1352.22). The three *D. pachea* strains were collected in 1996 in El Cardonal (Sonora, Mexico), in 1997 in Organ Pipe National Monument (Arizona, US) and in 2007 in Punta Ohna (Sonora, Mexico). Flies were raised at 25°C on standard medium containing 83 g of dry baker's yeast, 83 g of maize flour, 11 g of agar and 25 mL of 10% methyl 4-hydroxybenzoate (dissolved in ethanol) in 1 L of water. Tubes containing standard fly food (10 g) were supplemented with 60 microliters of a 5-mg/mL 7DHC (Sigma, Saint Louis) solution or of a 1-mg/mL lathosterol (Sigma) solution. *D. melanogaster* transgenic flies were produced by FlyFacility, Clermont-Ferrand. For the rescue experiment, we scored progeny flies according to sex and visible markers from more than 8 vials per food condition and per cross. More than 1000 progeny flies were scored in total for each condition.

Sequencing of the *nvd* locus

We used degenerate primers, inverse PCR, RT-PCR, 5' RACE and 3' RACE to sequence the *nvd* locus in various *Drosophila* species. To avoid potential PCR-induced errors, we determined DNA sequences from at least two independent PCR amplifications. See fig. S1 and Table S1 for amplification reactions and primers. Genomic DNA was isolated from adults using QIAgen DNeasy Tissue kit. Part of exon 2 was amplified from *D. acanthoptera* with primers nvd.ex2.F1 and nvd.ex2.R2. Part of exon 2 was amplified from all the other *nannoptera* group species and from *D. robusta* with nvd.ex2.F1 and nvd.ex2.R1 primers. Part of exon 3 was amplified from *D. pachea* with primers nvd.ex3.F1 and nvd.ex3.R1. Part of exons 5 and 6 was amplified from *D. pachea* with nvd.ex5.F1 and nvd.ex6.R2 primers, and from *D. acanthoptera* with nvd.ex5.F1 and nvd.ex6.R3 primers. PCR fragments were purified and cloned into PGEMT-Easy (Promega, Madison) prior to sequencing. RT-PCR showed that the three non overlapping *nvd* exonic sequences that we amplified using degenerate primers in *D. pachea* were contiguous, suggesting that a single *nvd* gene is present in the *D. pachea* genome. Inverse PCR was performed to amplify the 5' and 3' *nvd* regions from *D. pachea* and *D. acanthoptera*. Genomic DNA was digested with MspI or Sau3AI and then ligated using T4 ligase (Promega) (19). Total RNA was isolated from adults using SV Total RNA Isolation System (Promega) following the manufacturer's protocol. Reverse transcriptase reaction was performed with M-MLV retrotranscriptase (Promega) and oligo-dT primers. Subsequent 5' and 3' RACE were done using SMART™ RACE cDNA Amplification Kit (Clontech, Mountain View). Various PCR and RT-PCR were also performed to

sequence the entire *nvd* locus (fig. S1). For population genetics analysis, DNA was isolated from single flies with the QIAgen DNeasy Tissue kit and the 3-kb *nvd* locus was amplified and sequenced using the primers reported in Table S1.

Analysis of *nvd* coding sequences in Diptera species

Insect *nvd* gene regions were retrieved from NCBI database with TBLASTN and were annotated manually with Artemis (*20*). 5' RACE was performed as described above on *D. mojavensis* with the 5'Nvd-mojR primer and corroborated our gene annotation. Presumptive deleterious mutations were detected with SIFT (*21*) based on *Drosophila* and other insect NVD protein sequences. DNA sequences were aligned with ClustalW in BioEdit (*22*), with hand alignment of small indels based on amino acid sequences. Bayesian reconstruction of ancestral sequences and maximum likelihood analysis was performed with codeml in the PAML 4.2b package (*23*). We used the F3x4 model of codon frequencies. Global replacement changes per site (dN) / synonymous changes per site (dS) were calculated by a free-ratio model, which allows dN/dS to vary along different branches. To test whether the dN/dS ratio is higher in the *D. pachea* lineage, we used a branch model, where the null model is a single dN/dS ratio over the entire tree and the alternative model is two dN/dSs, one for the *D. pachea* lineage and one for the rest of the tree (Table S3).

In situ hybridization

Part of the *nvd* coding region was amplified by RT-PCR from *D. pachea*, *D.*

acanthoptera and *D. melanogaster* using the following primers: pa.ex2.F3 and pa.finR, ac.ex2.F3 and ac.finR, Nvd.up2 and Nvd.do2 respectively. Fragments were purified, cloned into pGEMT-Easy and sequenced. The resulting plasmids were digested with ApaI or SacI and used as templates to generate sense and anti-sense in situ probes using the dNTP DIG RNA labeling mix (Roche) with T7 or SP6 polymerases (Promega). Wandering third instar larvae were dissected in PBT and fixed in 4% paraformaldehyde. In situ hybridization was carried out according to standard protocols.

Steroid hormone extraction and HPLC separation

D. pachea flies were raised on regular fly food supplemented with 7DHC or with senita cactus pieces (see Methods section). For each condition, 100 wandering third instar larvae were homogenized in methanol and processed as described previously (*13*). Samples were then dissolved in HPLC mobile phase (a mix of dichloromethane/propan-2-ol/water, 125:30:1, v/v/v) and separated through a Zorbax® Sil column (250 x 4.6 mm i.d.) in an isocratic normal-phase mode using a Beckman HPLC apparatus (System Gold), a 1 mL min^{-1} flow rate and UV detection at 245 nm. From each collected fraction (700 microliters) we kept 175 microliters for nanoLC-MS/MS analyses and used the remaining part for enzyme immunoassay (EIA) detection of steroid hormones. All samples were evaporated to dryness.

Enzyme immunoassay detection of steroid hormones

Steroid hormones were detected with an enzyme immunoassay as described previously

(*13*). We used the polyclonal anti-ecdysone antiserum L2 (from M. De Reggi, Marseille), which displays the following cross-reactivities for reference steroids: ecdysone, 1.0 ; 20-hydroxyecdysone, 4.6 ; makisterone A, 50.0; makisterone C, 114.6. Calibration curves were generated with 20-hydroxyecdysone and results are given in 20-hydroxyecdysone equivalents.

NanoLC-tandem mass spectrometry

For nanoLC-MS/MS analyses, HPLC fractions corresponding to the two major immunoreactive peaks detected by EIA were pooled. Five fractions around the retention time of reference makisterone C were added to the pool of ecdysone/makisterone A zone fractions (see horizontal bars in fig. S5). Nano LC-MS/MS was performed at UPMC (Plate-forme de Spectrométrie de Masse et Protéomique, IFR 83, Paris) as described previously (*13*). Reference 20-hydroxyecdysone was given by J. Harmatha (Prague). Reference makisterone A and makisterone C were previously isolated from *Ajuga iva* (*24*) and *Leuzea carthamoides* (*25*), respectively. Reference ecdysone was purchased from Northern Biochemical Company, Russia. Their purity was higher than 97%.

Construction of plasmids for in vivo and in vitro assays

The *pUAST*, *pUAST-HA*, *UAS-GFP* and *UAS-HA-nvd-B.mori* plasmids were described previously (*8*, *15*, 26). The entire *nvd* coding region was amplified from *D. pachea*, *D. acanthoptera* and *D. mojavensis* cDNA using the following primers: pa-debut and pa-stop, ac-debut and ac-stop, moj-debut and moj-stop, respectively. Fragments were

subcloned into pGEMT-Easy, digested with *EcoR*I and *Kpn*I (*D. pachea*) or *Xho*I and *Xba*I (*D. acanthoptera*) or *Bgl*II and *Xba*I (*D. mojavensis*), and ligated into pUAST. The resulting *pUAS-nvd-D. mojavensis* plasmid contains part of the endogenous *nvd* 5' UTR. This construct gave the strongest NVD activity in our assay and was used as a reference in all our assays. A *pUAS-nvd-D. mojavensis* plasmid with no *nvd* 5'UTR was constructed using debut_pUAST3H_Dmoj_BamHI and pUASTR primers to amplify the *nvd* coding region and *Bgl*II/*BamH*I and *Xba*I as cloning sites into *pUAST*. The pGEMT-Easy vectors containing *nvd* inserts were used as templates for site-directed mutagenesis and mutants were generated with the QuickChange® Multi Site-Directed Mutagenesis kit according to the manufacturer's specifications (Stratagene, Europe). Primer sequences are indicated in Table S1. Then *nvd* inserts containing the mutations of interest were cloned into *pUAST*. *D. pachea HA-nvd* and *D. mojavensis HA-nvd* were amplified from *pUAST-nvd* constructs using the reverse primer pUASTR and a gene-specific forward primer (pacHAdebut and mojHAdebut), introducing a *BamH*I restriction site upstream of the start codon. The resulting PCR fragments were ligated into pGEMT, digested with *BamH*I and *Xba*I, and ligated into *pUAST-HA* linearized with *Bgl*II and *Xba*I. For preparation of HA-tagged *D. mojavensis nvd* constructs with mutations, pUAST-*D. mojavensis HA-nvd* was digested with *EcoR*I, releasing a HAtag-5´*nvd* coding sequence fragment and this fragment was ligated into the five *pUAST-D. mojavensis HA-nvd* constructs with mutations *using the EcoR*I site. For preparation of HA-tagged *D. pachea nvd* constructs with mutations, the same strategy was used, but digesting with *RsrI*I and *Xba*I. The *D. melanogaster Start1* cDNA was cloned as a *Xho*I-*Nhe*I fragment into the S2

expression vector *pBRAcpA* (from L. Cherbas), which contains an *actin5C* promoter. Maxiprep were performed using PureYield Plasmid Maxiprep System (Promega) following the manufacturer's instructions.

In vitro assay

Our assay was adapted from refs. (*15*, *27*). *D. melanogaster* S2 cells were maintained at 22 °C in Schneider medium (Invitrogen) supplemented with 10% heat-inactivated FCS and antibiotics (100 µg/mL streptomycin and 60 µg/mL penicillin). One day after subculture, cells were transfected using Effectene transfection reagent (QIAgen) with the following three plasmids: A*ctin5C-GAL4* (from Yasushi Hiromi), *UAS-GFP* (*26*), *Actin5C*-Start1 (*28*), and one of our *UAS-nvd* plasmids. GFP served as a control for transfection efficiency. Transfected cells were incubated for 3 days at 22 °C to allow optimal protein expression. Then, 4 mL-cell culture solutions were incubated with 80 microliters of a cholesterol or lathosterol solution (1 mg/mL in 45% 2-hydroxypropyl-β-cyclodextrin) for 24 h. Both 2-hydroxypropyl-β-cyclodextrin (Sigma) and *Actin5C-Start1*-transfection are thought to facilitate cholesterol absorption (*28*, *29*). Ethyl acetate extracts were analyzed by reverse phase-high pressure liquid chromatography (RP-HPLC) with a Waters 1525 HPLC system or an Ettan LC system. Conditions were as follows: C18 column (150 × 4.6 mm i.d. Advanced Chromatography Technologies), acetonitrile:isopropanol (5:2, vol/vol) solvent, 1 mL/min flow-rate, detection at 210 nm and 280 nm. NVD activity was measured as the amount of 7DHC produced (proportional to the corresponding peak surface). Since cell conditions can vary from day to day, the

amount of 7DHC was always reported relative to the amount of 7DHC produced by cells transfected during the same assay with the very active *UAS-nvd-D. moj* construct. This construct contains part of the *D. mojavensis nvd 5*'UTR upstream of the start codon. At least three independent assays were performed for each condition.

Western blot

For each sample we used 1 mL of transfected S2 cell culture after sterol addition and just before sterol extraction. Cells were pelleted, resuspended in PBS buffer, pelleted again and resuspended in 1 mL RIPA buffer (50 mM Tris-Cl pH 7.4, 150 mM NaCl, 1% NP-40, 0.5% Na Deoxycholate, 0.1% SDS, protease inhibitors). Cell extracts were sonicated with three 5-s pulses at output level 2 using a Branson sonifier S-250 with a 3-mm microtip. Standard Western blot protocols were applied for detection of epitope tagged NVD enzyme and actin using the following antibodies: rat anti-HA monoclonal antibody 11867423001 (Roche) (1:2000 dilution), donkey anti-rat peroxydase 31470 (Pierce) (1:1000 dilution), mouse anti-actin monoclonal antibody 691001 (MP Biomedicals) (1:2000 dilution), anti-mouse IgG peroxydase A6782 (Sigma) (1:1000 dilution).

Fluorescent in situ hybridization (FISH) of polytene chromosomes

Polytene chromosomes were prepared from *D. pachea* 15090-1698.02 third instar larva salivary glands by standard acid fixation squash procedures (*30*). For fixation, salivary glands were incubated in 45% acetic acid for 5 min, and then in 50% acetic acid and 16,67% lactic acid for 2 min. FISH probes were prepared with the FISH Tag DNA Green

Kit, Alexa Fluor 488 (Life Technologies). Each labeling was performed with an equimolar pool of five 1.5-to-2.5-kb PCR products corresponding to the amplification of 8 to 10 kb of the genomic region of interest (see Table S1 for primers). Hybridization of DNA probes to polytene chromosomes was carried out following the protocol of (*30*). As a control, we stained for the *Acetyl-CoA carboxylase* (*ACC*) locus in *D. pachea* and we observed that it localizes to a polytene band that is different from the one detected with the *nvd* probe (not shown).

D. pachea whole genome sequencing and assembly

The DNA of thirty individuals of the *D. pachea* 15090-1698.02 line was sequenced with the Illumina platform (Fasteris, Geneva, 2x100 bp, 134 million reads). The genome sequence was assembled with velvet 1.0.13 (*31*) using multiple hash lengths (k = 45, 49, 53, 57, 63). The assembly based on 49-kmers was chosen for further analysis. The N50 contig length of this assembly is 3,661 bp (minimum contig size = 100 bp). Then, 8 kb- and 20 kb- Long Jumping Distance (LJD) libraries (Eurofins MWG, Ebersberg) were constructed from a pool of genomic DNA from 120 adults of the *D. pachea* 5090-1698.02 line and sequenced with the Illumina platform (2x100 bp, 33 millions of reads paired with another read for the 8 kb-library and 33 million of reads paired with another read for the 20 kb-library). Reads were mapped to the genome assembly with bwa 0.5.5 (*32*). The mapping results were visualized with IGV (*33*) and contigs adjacent to the contig containing *nvd* were linked manually based on the LJD paired-end read information. This method allowed us to obtain a scaffold spanning approximately 40 kb

on the 3' side of *nvd* and more than 150 kb on the other side (fig. S9). A better assembly of the *D. pachea* genome sequence is ongoing and will be published elsewhere. For gene annotation, we performed BLAST searches in Drosophila nucleotide sequences with tblastx and blastn and annotated coding sequences manually in Geneious (*34*).

Natural population sampling and initial processing of population genetics sequence data

Initially, we collected a population of 15 individuals from Guaymas (Sonora, Mexico) in 2003 and another one of 14 individuals from San Felipe (Baja California, Mexico) in 2008. On May 2011, we placed two bottles containing rotten senita cactus in a large cactus forest near San Felipe (Baja California, Mexico 114 53' 40.26" W, 31 06' 20.71" N). On May 14 we collected 34 *D. pachea* individuals: 13 were found in one bottle and 21 in another bottle located 5 meters away. We recorded the sex of each individual (Table S4). Genomic DNA was isolated from each individual fly using QIAgen DNeasy Tissue kit. The 3-kb- *nvd* locus (from the start codon to the stop codon, including introns) was amplified and Sanger-sequenced in all the individuals (see Table S1 for primers). In addition, we amplified and sequenced seven genes located in the scaffold containing *nvd* and nine “control” genes that were chosen randomly across the genome from the 34 individuals collected in 2011 (fig. 4). The PCR amplicon length ranged from 1.5 to 3.5 kb and was sequenced with at least two sequencing primers (Table S1). We used Geneious 5.5.6 (*34*) and Indelligent (*35*) to find heterozygote nucleotide positions and infer heterozygote indels. Loci with heterozygote SNPs in males were inferred to be autosomal

(*acc, ddc, pis, RhoI, sad, Tpi* and all the genes in the *nvd* scaffold) whereas loci with no heterozygote nucleotides in males were inferred to be X-linked (*dib, shade, smt3*). Indels were removed manually from all the sequences. The sequences were then phased using the Stephens et al. PHASE tool (*36*), and the resulting haplotypes (68 haplotypes for each autosomal gene and 59 haplotypes for X-linked genes) were used in subsequent analysis.

Population Structure

If the San Felipe sample of 34 individuals came from a highly structured population, this could present a challenge in interpretation of the other population genetic analysis. The control region data were subjected to analysis using STRUCTURE (*37*) and we also applied Principal Components Analysis (*38*) to assess whether these data look like a single panmictic population. We found no hint of clustering of any subset of lines (fig. S10), in agreement with the results of STRUCTURE (not shown), indicating no sign that this population has significant substructure. For subsequent analysis, we accepted the null hypothesis that the data behave as though the 34 sampled individuals are derived from a single panmictic population.

Population genetics analysis

The estimates of the population recombination rate, rho = 4Nr, were calculated with DnaSP (*39*) and compared between the *nvd* region and the control regions (Table S7). The counts of synonymous differences, nonsynonymous differences and rate of substitutions per nonsynonymous site (Ka) were done with DnaSP (Table S8). We also

on the 3' side of *nvd* and more than 150 kb on the other side (fig. S9). A better assembly of the *D. pachea* genome sequence is ongoing and will be published elsewhere. For gene annotation, we performed BLAST searches in Drosophila nucleotide sequences with tblastx and blastn and annotated coding sequences manually in Geneious (*34*).

Natural population sampling and initial processing of population genetics sequence data

Initially, we collected a population of 15 individuals from Guaymas (Sonora, Mexico) in 2003 and another one of 14 individuals from San Felipe (Baja California, Mexico) in 2008. On May 2011, we placed two bottles containing rotten senita cactus in a large cactus forest near San Felipe (Baja California, Mexico 114 53' 40.26" W, 31 06' 20.71" N). On May 14 we collected 34 *D. pachea* individuals: 13 were found in one bottle and 21 in another bottle located 5 meters away. We recorded the sex of each individual (Table S4). Genomic DNA was isolated from each individual fly using QIAgen DNeasy Tissue kit. The 3-kb- *nvd* locus (from the start codon to the stop codon, including introns) was amplified and Sanger-sequenced in all the individuals (see Table S1 for primers). In addition, we amplified and sequenced seven genes located in the scaffold containing *nvd* and nine “control” genes that were chosen randomly across the genome from the 34 individuals collected in 2011 (fig. 4). The PCR amplicon length ranged from 1.5 to 3.5 kb and was sequenced with at least two sequencing primers (Table S1). We used Geneious 5.5.6 (*34*) and Indelligent (*35*) to find heterozygote nucleotide positions and infer heterozygote indels. Loci with heterozygote SNPs in males were inferred to be autosomal

(*acc, ddc, pis, RhoI, sad, Tpi* and all the genes in the *nvd* scaffold) whereas loci with no heterozygote nucleotides in males were inferred to be X-linked (*dib, shade, smt3*). Indels were removed manually from all the sequences. The sequences were then phased using the Stephens et al. PHASE tool (*36*), and the resulting haplotypes (68 haplotypes for each autosomal gene and 59 haplotypes for X-linked genes) were used in subsequent analysis.

Population Structure

If the San Felipe sample of 34 individuals came from a highly structured population, this could present a challenge in interpretation of the other population genetic analysis. The control region data were subjected to analysis using STRUCTURE (*37*) and we also applied Principal Components Analysis (*38*) to assess whether these data look like a single panmictic population. We found no hint of clustering of any subset of lines (fig. S10), in agreement with the results of STRUCTURE (not shown), indicating no sign that this population has significant substructure. For subsequent analysis, we accepted the null hypothesis that the data behave as though the 34 sampled individuals are derived from a single panmictic population.

Population genetics analysis

The estimates of the population recombination rate, rho = 4Nr, were calculated with DnaSP (*39*) and compared between the *nvd* region and the control regions (Table S7). The counts of synonymous differences, nonsynonymous differences and rate of substitutions per nonsynonymous site (Ka) were done with DnaSP (Table S8). We also

performed two tests of selection that rely on the consistency of polymorphism and divergence at synonymous and nonsynonymous sites. The McDonald-Kreitman test (*40*) tabulates the counts of synonymous and nonsynonymous polymorphic sites and compares them to the counts of synonymous and nonsynonymous divergent sites when *D. pachea* sequences are compared to an outgroup (*D. mojavensis*). The McDonald-Kreitman test asks whether the pattern of polymorphism is consistent with the pattern of divergence (Table S9). The other test that was applied, the Hudson-Kreitman-Aguadé test (*41*), also uses a contrast between levels of polymorphism and divergence. This test fits a model consistent with the observed nucleotide diversity and asks about the consistency of nucleotide divergence at two genomic regions. We contrasted the *nvd* region to the control regions using the HKA test. This test shows that the *nvd* region has less polymorphism than the control loci, despite the fact that the divergence (and hence mutation rates) are similar. The HKA test yielded a chi-square of 18.348, and a P-value of 10^{-4}.

The Kim and Nielsen omega statistics (*42*, *43*), which tests for selective sweeps, was calculated with the OmegaPlus sofware (*44*). The plot was made as though there is no gap between genes, which is somewhat artificial but is justified by the fact that there is such a low rate of recombination (fig. 4). We performed 1000 simulations using the neutral coalescent simulator ms (*45*) and the average estimates of theta and rho for the region in order to calculate the significance level of omega (fig. 4). We conclude that there is evidence of at least one selective sweep in the *nvd* region.

The haplotype bifurcation diagram was created with the SWEEP sofware developed by

the Broad Institute (*46*). Input data for SWEEP was the concatenated and phased data for the nvd region spanning from *C952* to *SpdS*. Linkage disequilibrium (LD) estimates were based on genotypic correlations calculated from unphased sequences using Zaykin's mcld program (*47*). The LD heat map was constructed using the LDheatmap R package (*48*).

Supporting Text

Lathosterol conversion

In mammals, lathosterol is converted into 7DHC during cholesterol biosynthesis by the Δ7-sterol C5-desaturase SC5DL (*49*). This desaturase is a membrane nonheme iron enzyme and is orthologous to the *Saccharomyces cerevisiae* ERG3 D5-desaturase involved in ergosterol biosynthesis (*49*), whereas NVD is a Rieske oxygenase (*8*). No ERG3 ortholog is present in any *Drosophila* species sequenced to date (*50*) and no NVD ortholog has yet been found in mammals (*8*, *15*). Our work thus suggests that conversion of lathosterol into 7DHC is catalyzed by unrelated enzymes in *Drosophila* and mammals.

Nvd and heterochromatin

In *D. melanogaster* the *nvd* gene is located in heterochromatin near the centromere on the left arm of chromosome 3 (*8*) whereas in *D. mojavensis* the *nvd* gene is located within one of the largest scaffolds, scaffold_6540, which is typical of euchromatin (*48*). The Y chromosome, the fourth chromosome and regions around centromeres and telomeres are typical heterochromatin domains in *Drosophila* (*49*). They are marked by HP1 protein and H3K9 methylation (*50*) and are characterized by low nucleotide diversity and low recombination rate (*51*). For several reasons we think that the low nucleotide diversity and low recombination rate we observed in the *nvd* region in *D. pachea* is not due to the fact that this gene is – or was very recently – in HP1 heterochromatin in *D. pachea*. First, our FISH analysis (fig. S12) shows that *nvd* is

located in the middle of a chromosome arm in *D. pachea*. Second, in *D. melanogaster*, the median intron length of euchromatic protein coding genes is 79 bp (*52*) and genes located in heterochromatin are in average four times larger than introns located in euchromatin (*53*). Intron size of the *nvd* gene in the *D. nannoptera* subgroup species and *D. mojavensis* is typical of euchromatin genes (fig. S11). Third, repetitive sequences typically reside within one or more introns of each gene as well as in intergenic regions in heterochromatin (*53*). No large repetitive sequences were found in our *nvd* scaffold of *D. pachea* and in the part of *D. mojavensis* scaffold_6450 that contains *nvd* and the neighboring orthologs.

However, we found that the %GC is significantly lower in the *nvd* region than in the control loci both in *D. mojavensis* and *D. pachea* (Table S9). In general, protein-coding genes in heterochromatin regions are approximatively 5–10% more AT-rich than their euchromatic orthologs in other *Drosophila* species (*53*). This suggests that *nvd* was embedded in heterochromatin in the past. According to the variation of intron sizes within the Drosophilidae phylogeny (fig. S11), *nvd* might have moved from heterochromatin to euchromatin before the separation of the *D. mojavensis* and *D. pachea* lineages. Translocations from heterochromatin to euchromatin and vice versa are not rare during Drosophila evolution (*51–53*).

Summary of the population genetics analysis of the *nvd* locus

Our population genetics analysis shows that *nvd* is in a large genomic region with low recombination rate and low nucleotide diversity. The divergence rate (between *D.*

mojavensis and *D. pachea*) of the coding sequences present in the *nvd* region is not significantly different from genes located in unlinked regions of the genome (Table S8). Regions of lower recombination rates are expected to diverge faster (*54*, *55*) but this is not the case here, suggesting that the low recombination rate and low nucleotide diversity of the *nvd* region is a relatively recent phenomena that appeared after the separation of the *D. mojavensis* and *D. pachea* lineages. Such a low diversity and recombination rate over several dozens of kilobases in a *Drosophila* species can be the result of recent and strong positive selection. The Kim and Stephen omega statistics does indeed show evidence for a selective sweep (fig. 4). A recent selective sweep would generate a strong linkage disequilibrium (LD) over a group of segregating sites, which is not the case here (fig. S13). The pattern of linkage disequilibrium that we observe (a low level of LD background with a few sites of high LD) rather suggests that the *nvd* region is recovering from one or several selective sweeps. Together, our data are consistent with an old selective sweep in a low recombination region, or with multiple recent selective sweeps targeting neighboring loci in the *nvd* region. Because of the low level of polymorphism of the *nvd* region, neither the date of the selective sweep nor the precise target gene of the selective sweep can be inferred.

Supporting figures

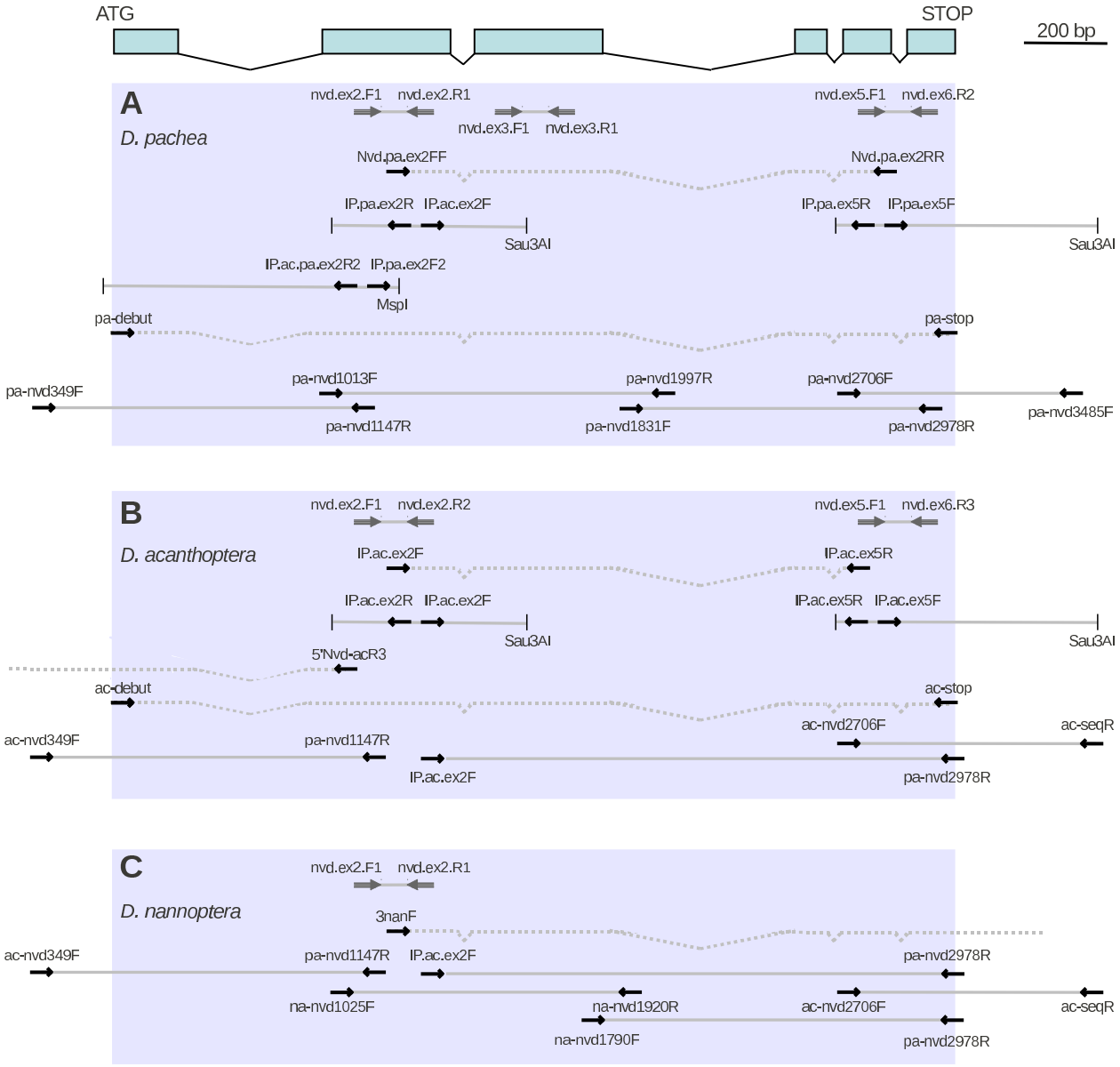

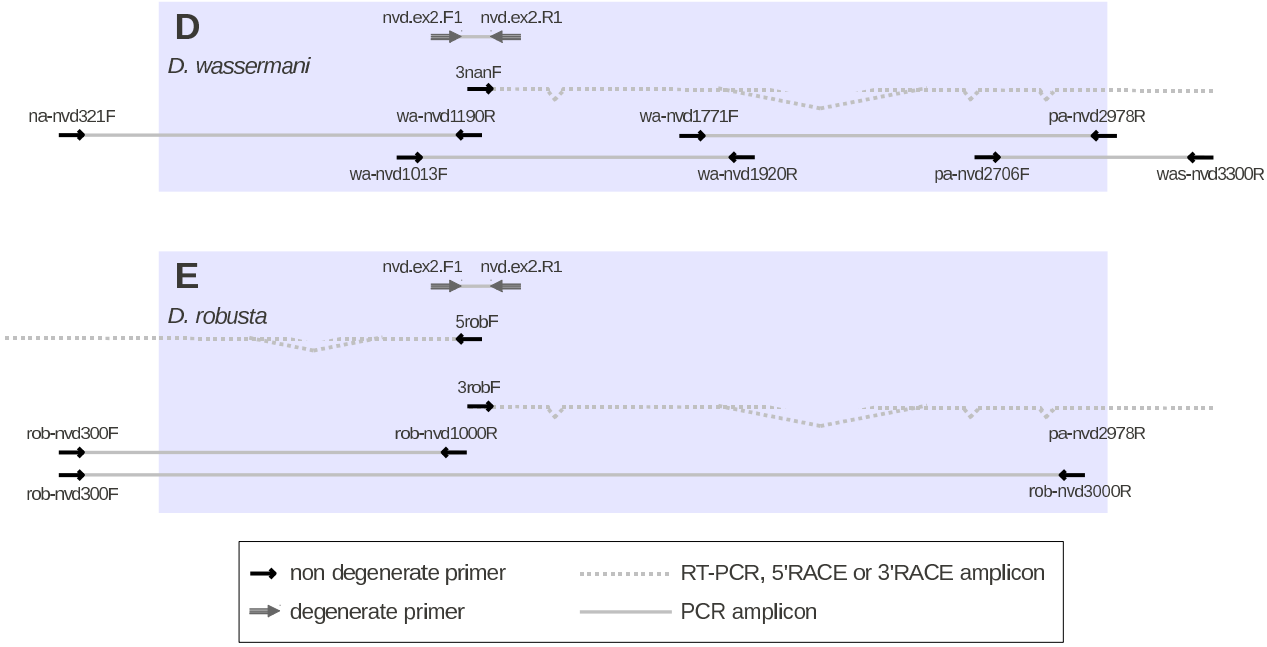

Figure S1. Schematic representation of the most representative amplification reactions performed in *D. pachea* (A), *D. acanthoptera* (B), *D. nannoptera* (C), *D. wassermani* (D) and *D. robusta* (E) to obtain *nvd* sequences. Schematic structure of the *nvd* gene is shown in the top panel, with blue boxes representing coding exons. Legend is indicated below.

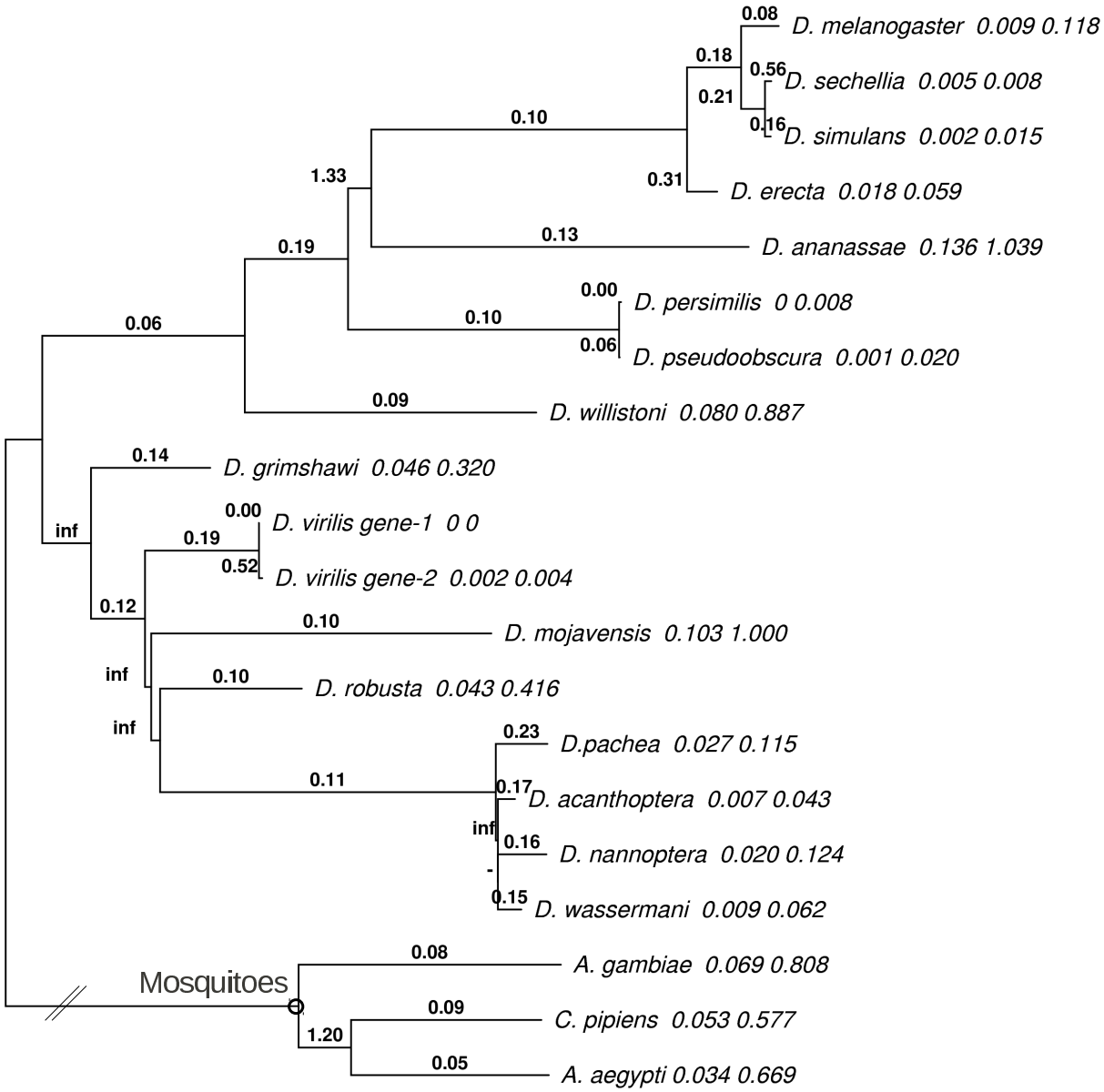

Figure S2. Phylogeny and dN/dS ratios of Diptera *nvd* sequences. Branch lengths are proportional to the number of nucleotide substitutions per codon (scale on the top left corner), except for the mosquitoes-Drosophila branch which should be 50 times longer. dN/dS values are shown in bold above each branch. "inf" refers to cases where dS equals or approximates 0. The dN and dS values corresponding to terminal branches are also indicated near each species name. Values were calculated with the free-ratio model and the F3x4 model of codon frequencies in PAML. The tree topology is based on refs (*55-57*).

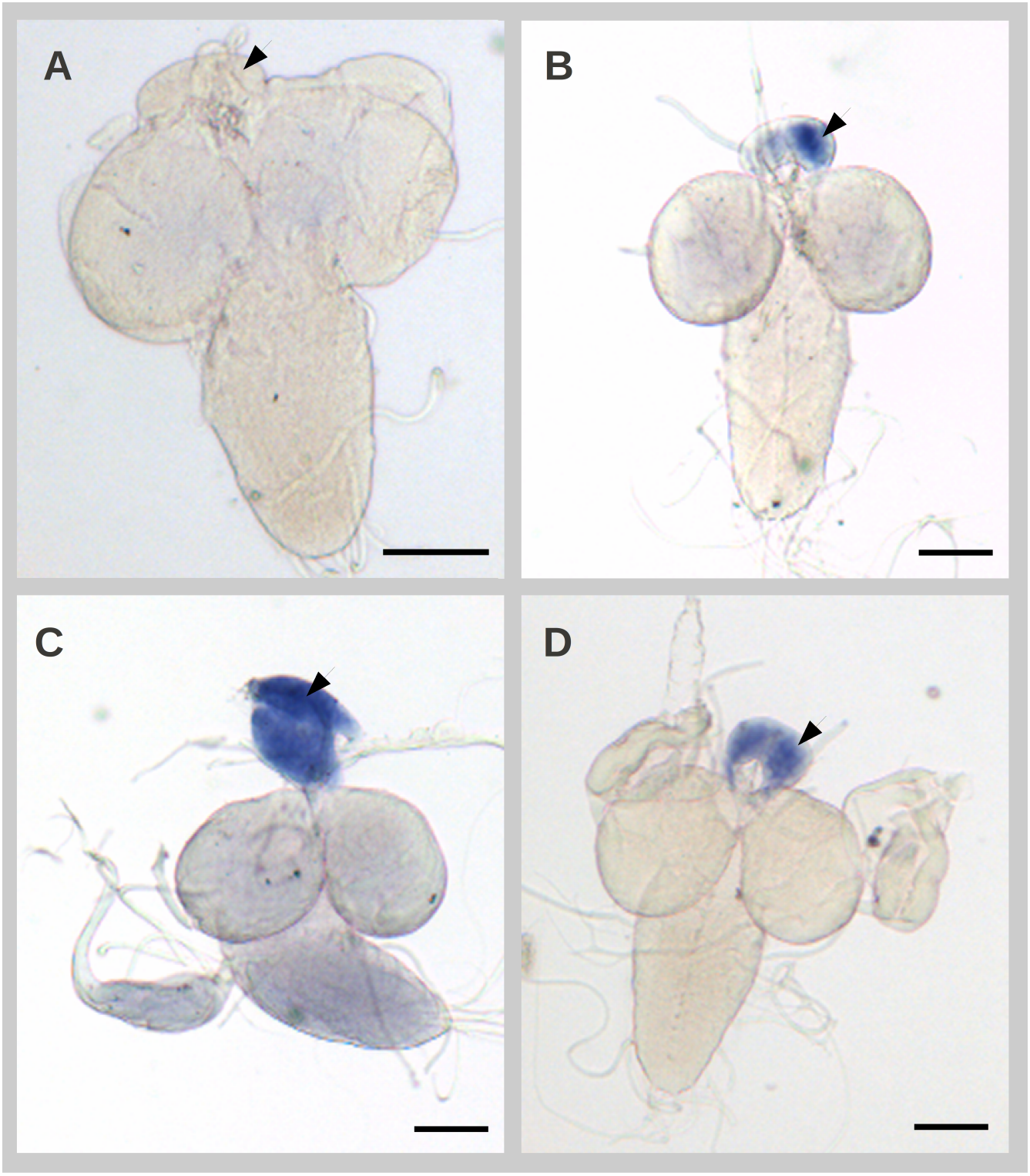

Figure S3. In situ hybridization of *nvd* in the brain-ring gland complex. *D. melanogaster* w^{1118} (A-B), *D. pachea* (C) and *D. acanthoptera* (D) third instar larvae at the wandering stage were stained with sense (A) or antisense (B-D) probe. *nvd* is expressed in the prothoracic gland. No *nvd* expression was detected in other larval tissues. Arrowheads point to the prothoracic gland. Scale bar is 100 µm.

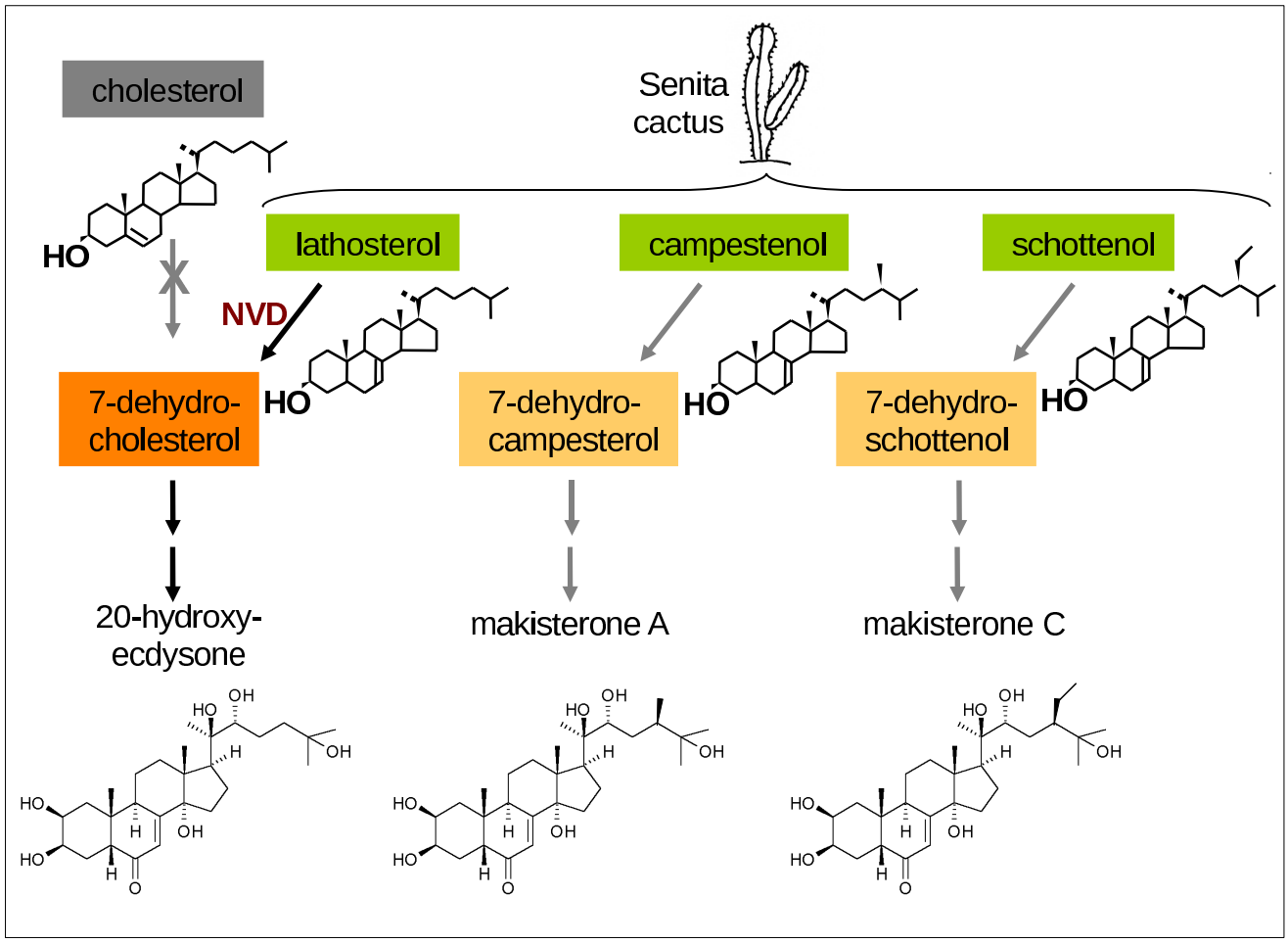

Figure S4. Putative *D. pachea* steroid hormone metabolic pathways. The senita cactus contains lathosterol, campestenol and schottenol as putative precursors (*7*). Owing to their inability to dealkylate 24-alkylsterols, insects are thought to produce various steroid hormones, depending on available dietary sterols (*13*).

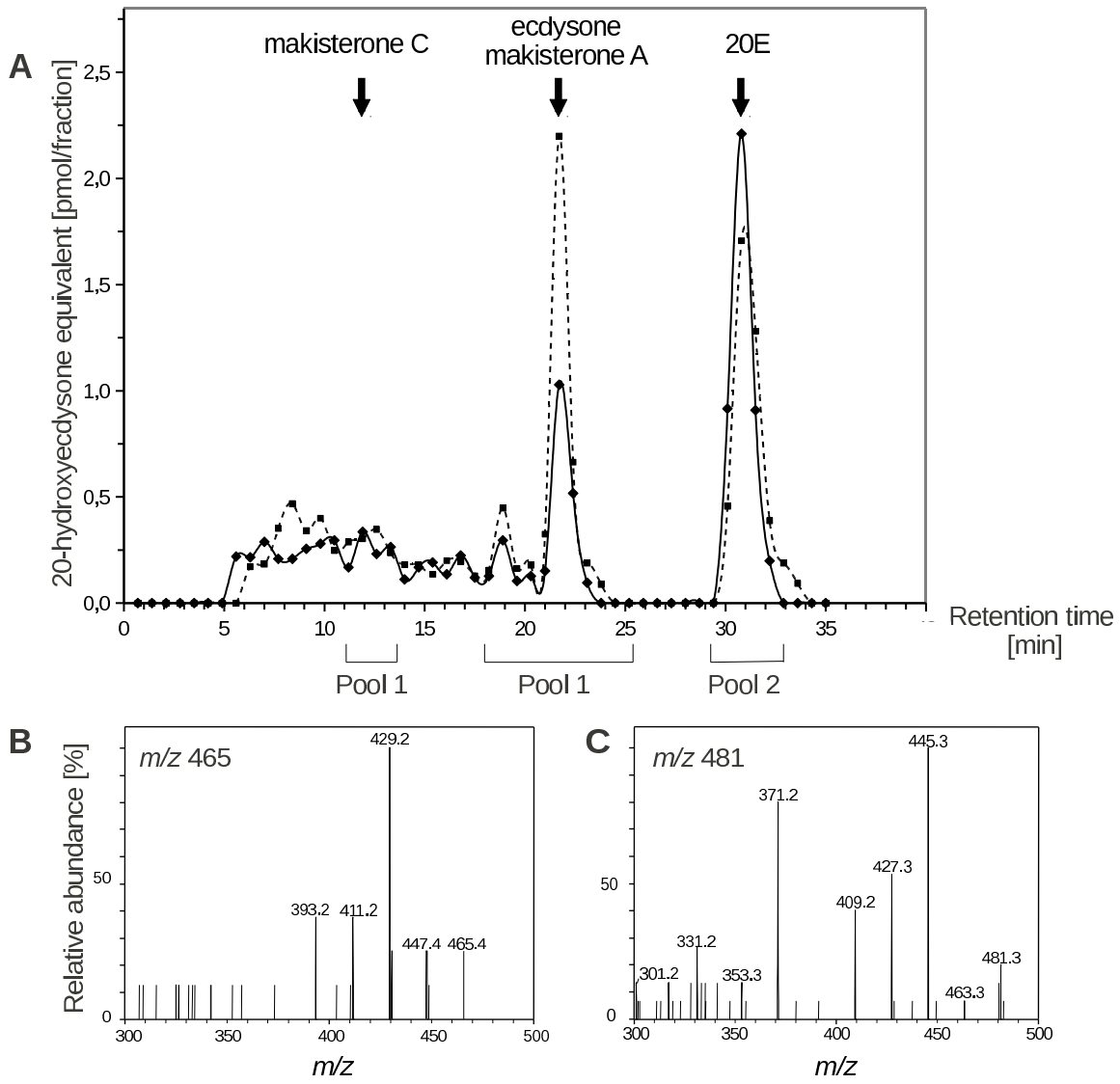

Figure S5. Biochemical analysis of *D. pachea* steroid hormones.A, NP-HPLC-EIA analysis of steroids extracted from *D. pachea* raised on regular fly food supplemented with senita cactus (black line) or with 7DHC (dotted line). Arrows indicate retention times of reference steroids. Ecdysone and makisterone A have the same retention time in this HPLC system. Brackets indicate fractions that were pooled and analyzed further by LC-MS/MS. (**B-C**) MS/MS spectra of steroids present in pooled HPLC fractions from *D. pachea* raised on senita cactus. **B**, MS/MS spectrum at *m/z* 465 from pool 1. This spectrum is similar to the MS/MS spectrum of ecdysone (*13*). No characteristic fragments corresponding to makisterone C or A at *m/z* 509 or 495, respectively, were detected. **C**, MS/MS spectrum at *m/z* 481 from pool 2. This spectrum is similar to the MS/MS spectrum of 20-hydroxyecdysone (*13*).

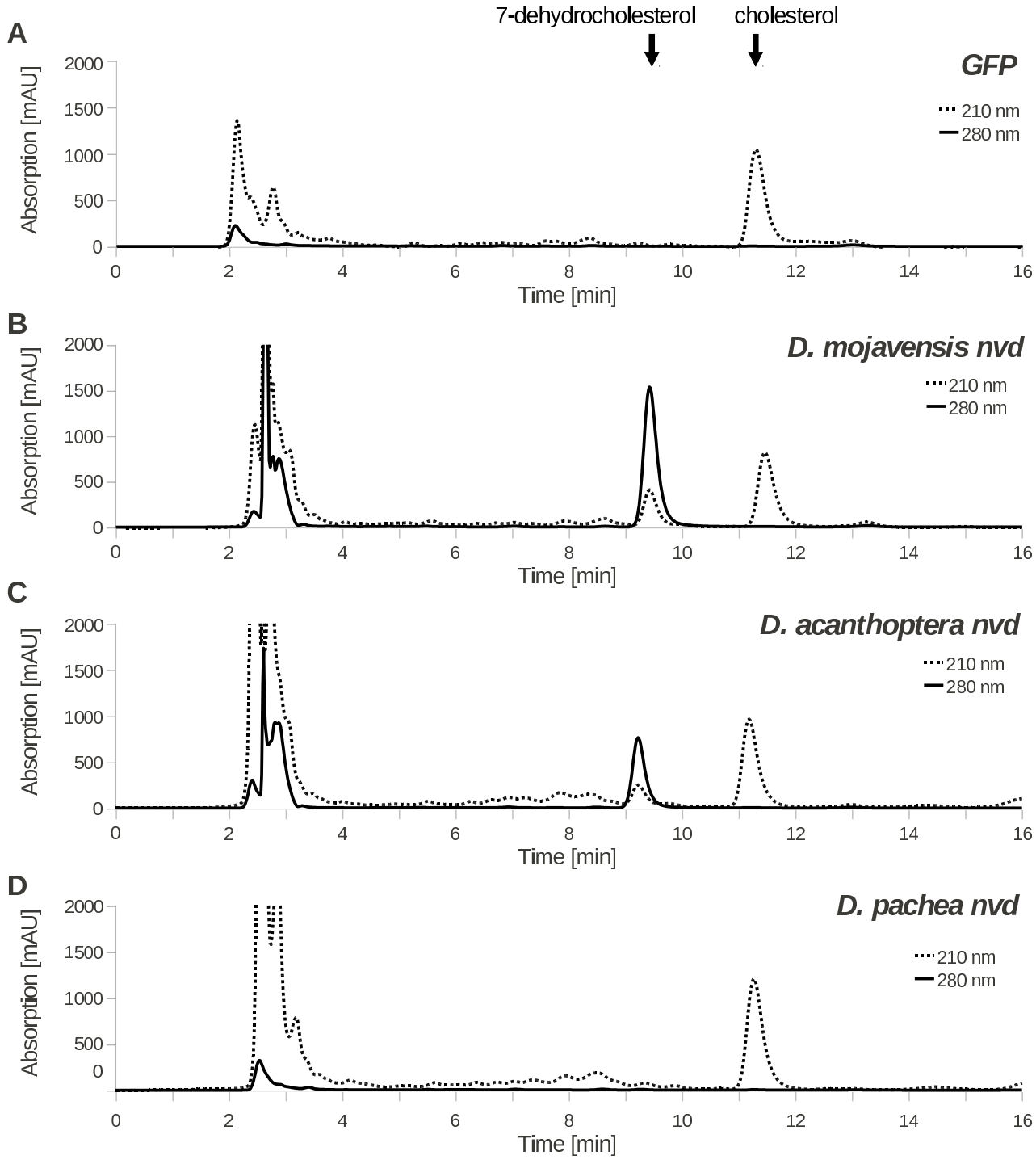

Figure S6. RP-HPLC analysis after S2 cell incubation with cholesterol. Cells were transfected with a *GFP* negative control (**A**), with *D. mojavensis nvd* (**B**), with *D. acanthoptera nvd* (**C**), or with *D. pachea nvd* (**D**). Absorption was measured at 280 nm (black line) and 210 nm (dotted line) simultaneously. Cholesterol absorbs preferentially at 210 nm and 7DHC at 280 nm. Retention time of cholesterol and 7DHC reference compounds are indicated with arrows. In our assays, *D. mojavensis* NVD typically converts about 20% of total cholesterol or lathosterol into 7-dehydrocholesterol.

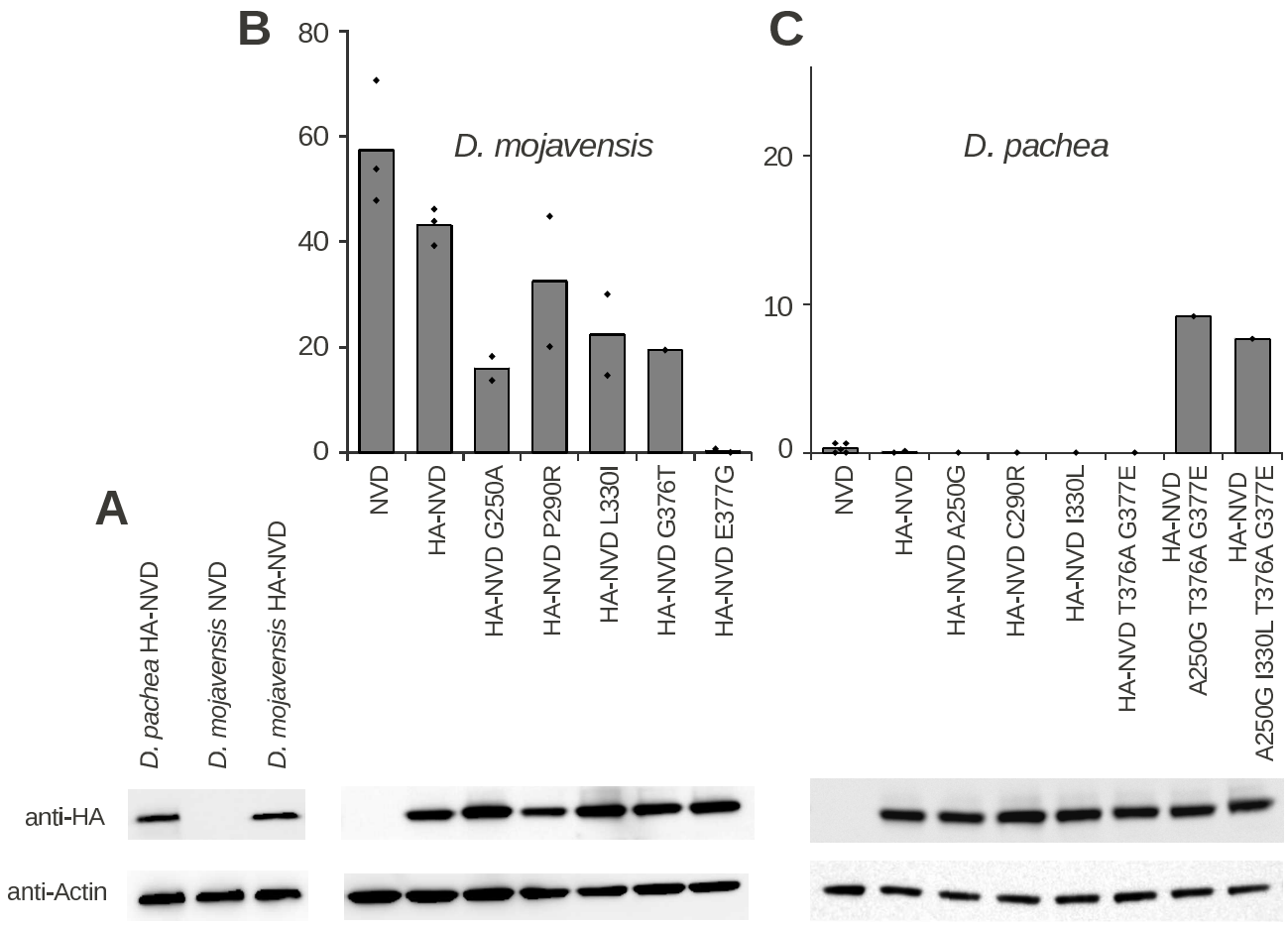

Figure S7. Expression of HA-tagged NVD proteins in the S2 cell NVD in vitro assay. (**A**) Western blot of *D. pachea* and *D. mojavensis* N-terminal HA-tagged NVD and *D. mojavensis* NVD without tag, using anti-HA and anti-Actin antibodies. Note that *D. pachea* HA-NVD is expressed at comparable levels to *D. mojavensis* HA-NVD. (**B,C**) Relative NVD enzyme activities of (**B**) *D. mojavensis* NVD, HA-NVD and HA-NVD with mutations and (**C**) *D. pachea* NVD, HA-NVD and HA-NVD with mutations; cholesterol was used as substrate. Western blots with anti-HA and anti-Actin are presented below for each expression assay. Protein extract corresponding to 10 microliters of homogenized cell culture was applied to each lane. NVD activity levels are indicated as in Fig. 3. Note that HA-tagged NVD proteins consistently display a lower enzymatic activity than wild-type NVD proteins. Nevertheless, the relative effects of the tested mutations are comparable between HA-tagged and non HA-tagged enzymes (compare Fig. 3B with S7B and 3C with S7C).

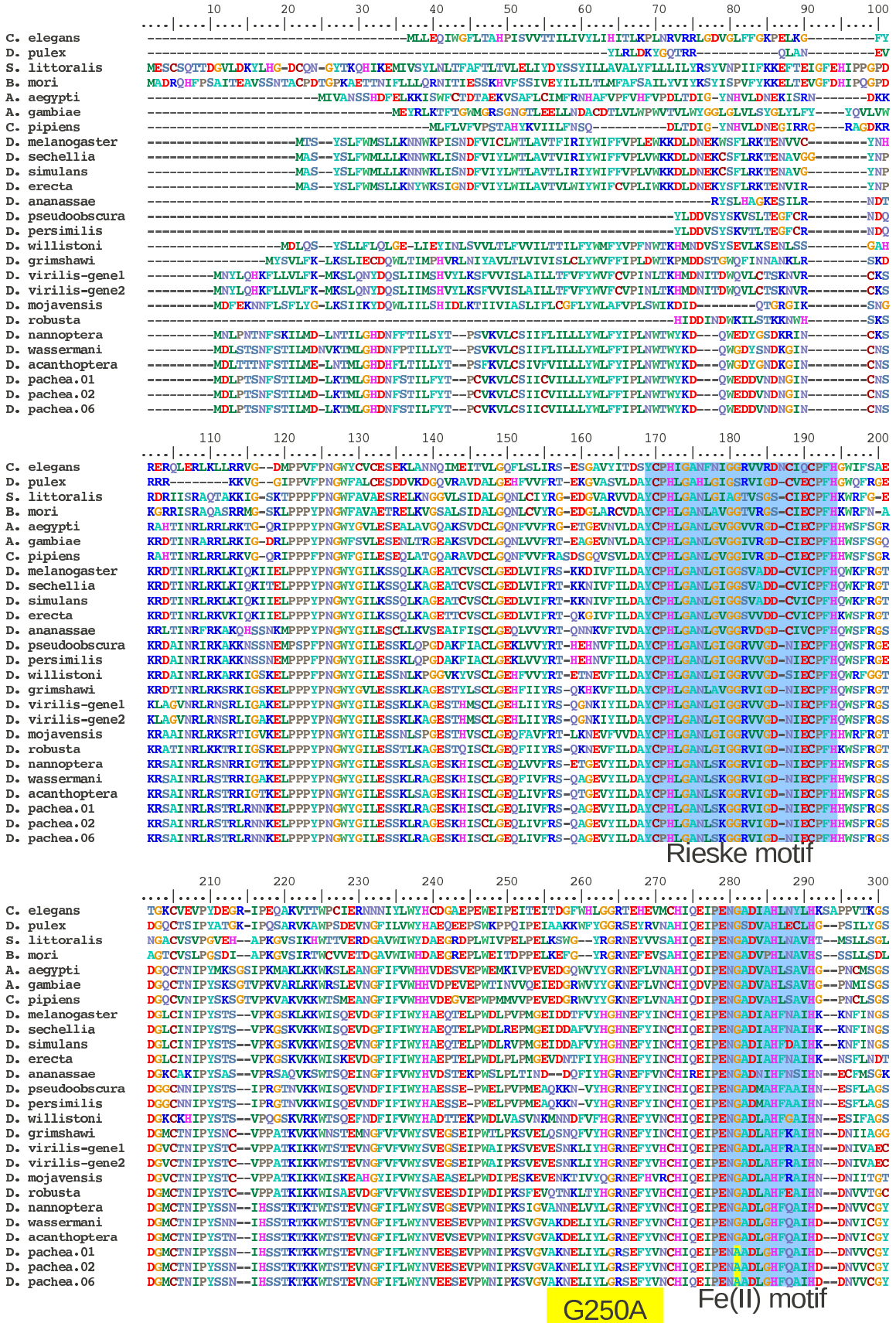
C. elegans
D. pulex
S. littoralis
B. mori
A. aegypti
A. gambiae
C. pipiens
D. melanogaster
D. sechellia
D. simulans
D. erecta
D. ananassae
D. pseudoobscura
D. persimilis
D. willistoni
D. grimshawi
D. virilis-gene1
D. virilis-gene2
D. mojavensis
D. robusta
D. nannoptera
D. wassermani
D. acanthoptera
D. pachea.01
D. pachea.02
D. pachea.06
Rieske motif
G250A
Fe(II) motif

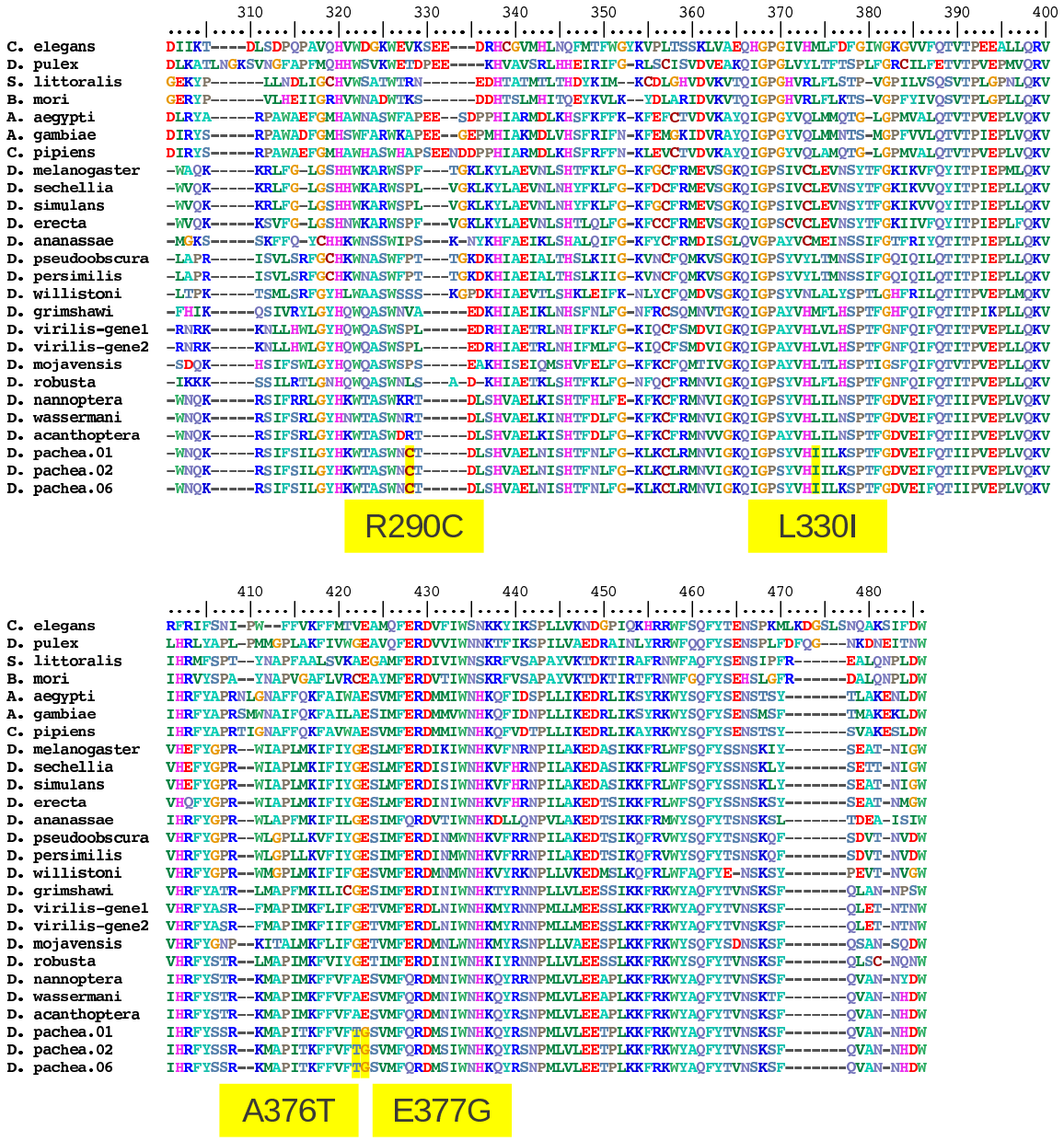

Figure S8. Alignment of NVD protein sequences from various *D. pachea* individuals and several insect species. The Rieske domains and the non-heme iron-binding domains are indicated in yellow. The five presumptive deleterious mutations detected with SIFT and tested in in vitro assays are in yellow.

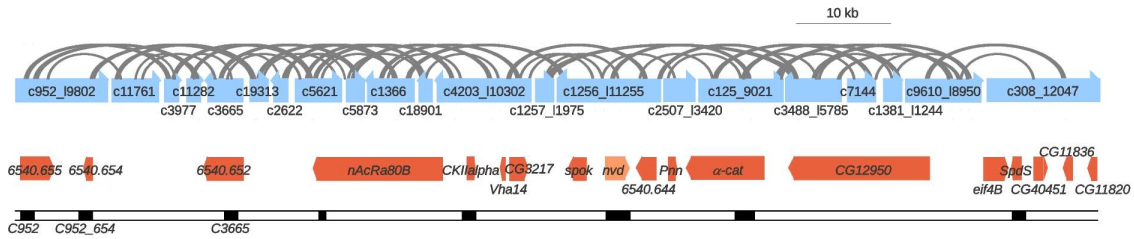

Figure S9. Reconstructed *D. pachea nvd* scaffold. Each contig is shown as a blue rectangle. Contigs were linked together when more than three non-overlapping reads were paired with reads mapping to another contig. Small brackets correspond to 8-kb-long jumping distance reads and large brackets to 20-kb-long jumping distance reads. Annotated genes are shown in red and orange. The PCR fragments that were sequenced for the population genetics analysis are indicated as black rectangles.

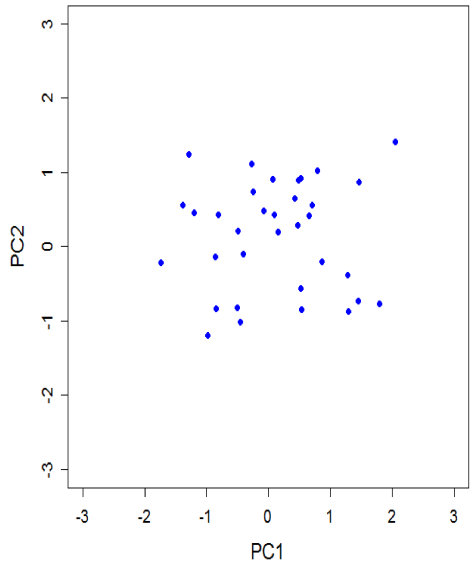

Figure S10. Principal Component Analysis of the sequences obtained from 34 *D. pachea* individuals. No clustering of any subset of lines is found, indicating that the population looks like a single panmictic population.

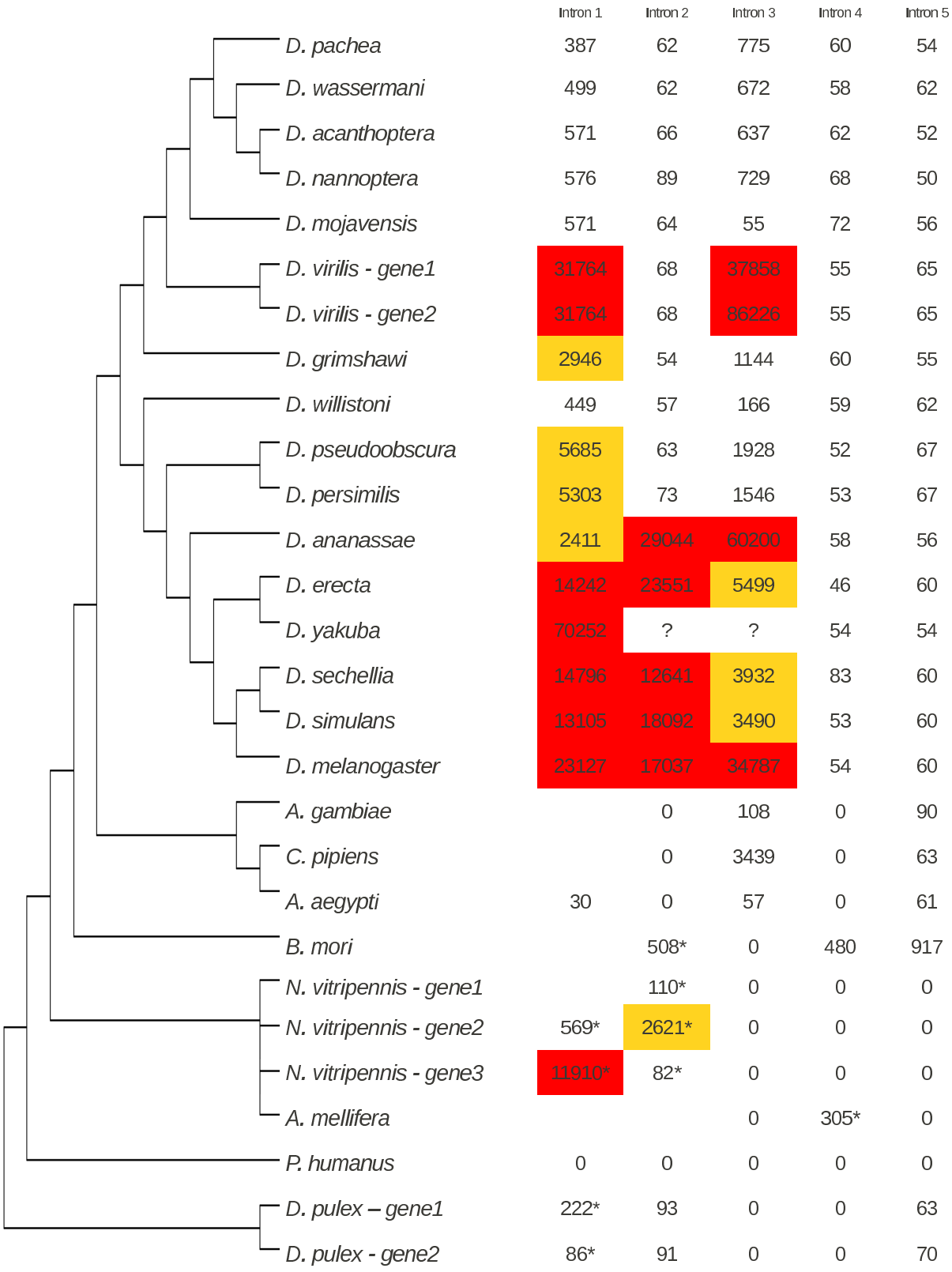

	Intron 1	Intron 2	Intron 3	Intron 4	Intron 5
D. pachea	387	62	775	60	54
D. wassermani	499	62	672	58	62
D. acanthoptera	571	66	637	62	52
D. nannoptera	576	89	729	68	50
D. mojavensis	571	64	55	72	56
D. virilis - gene1	31764	68	37858	55	65
D. virilis - gene2	31764	68	86226	55	65
D. grimshawi	2946	54	1144	60	55
D. willistoni	449	57	166	59	62
D. pseudoobscura	5685	63	1928	52	67
D. persimilis	5303	73	1546	53	67
D. ananassae	2411	29044	60200	58	56
D. erecta	14242	23551	5499	46	60
D. yakuba	70252	?	?	54	54
D. sechellia	14796	12641	3932	83	60
D. simulans	13105	18092	3490	53	60
D. melanogaster	23127	17037	34787	54	60
A. gambiae		0	108	0	90
C. pipiens		0	3439	0	63
A. aegypti	30	0	57	0	61
B. mori		508*	0	480	917
N. vitripennis - gene1		110*	0	0	0
N. vitripennis - gene2	569*	2621*	0	0	0
N. vitripennis - gene3	11910*	82*	0	0	0
A. mellifera			0	305*	0
P. humanus	0	0	0	0	0
D. pulex – gene1	222*	93	0	0	63
D. pulex - gene2	86*	91	0	0	70

Figure S11. Intron size of the *nvd* gene accross several insect species. The five introns of the *D. melanogaster nvd* gene are located at the following amino acid positions: first, 50; second, 180; third, 280; fourth, 319; fifth, 378. All are in phase 0 (splicing between codons) except the second and third intron which are in phase 1 (splicing between the first nucleotide of the codon and the second) and 2 (splicing between the second nucleotide of the codon and the third), respectively. * indicates introns which are located at a slightly different position and/or with another phase. ?: intron annotation is unclear. Introns whose size is greater than 2 kb are shown in yellow and those whose size is greater than 10 kb are in red. The *nvd* gene lies in heterochromatin in *D. melanogaster* (*7*). Transitions between small size and large size introns might be associated with euchromatin-heterochromatin translocations.

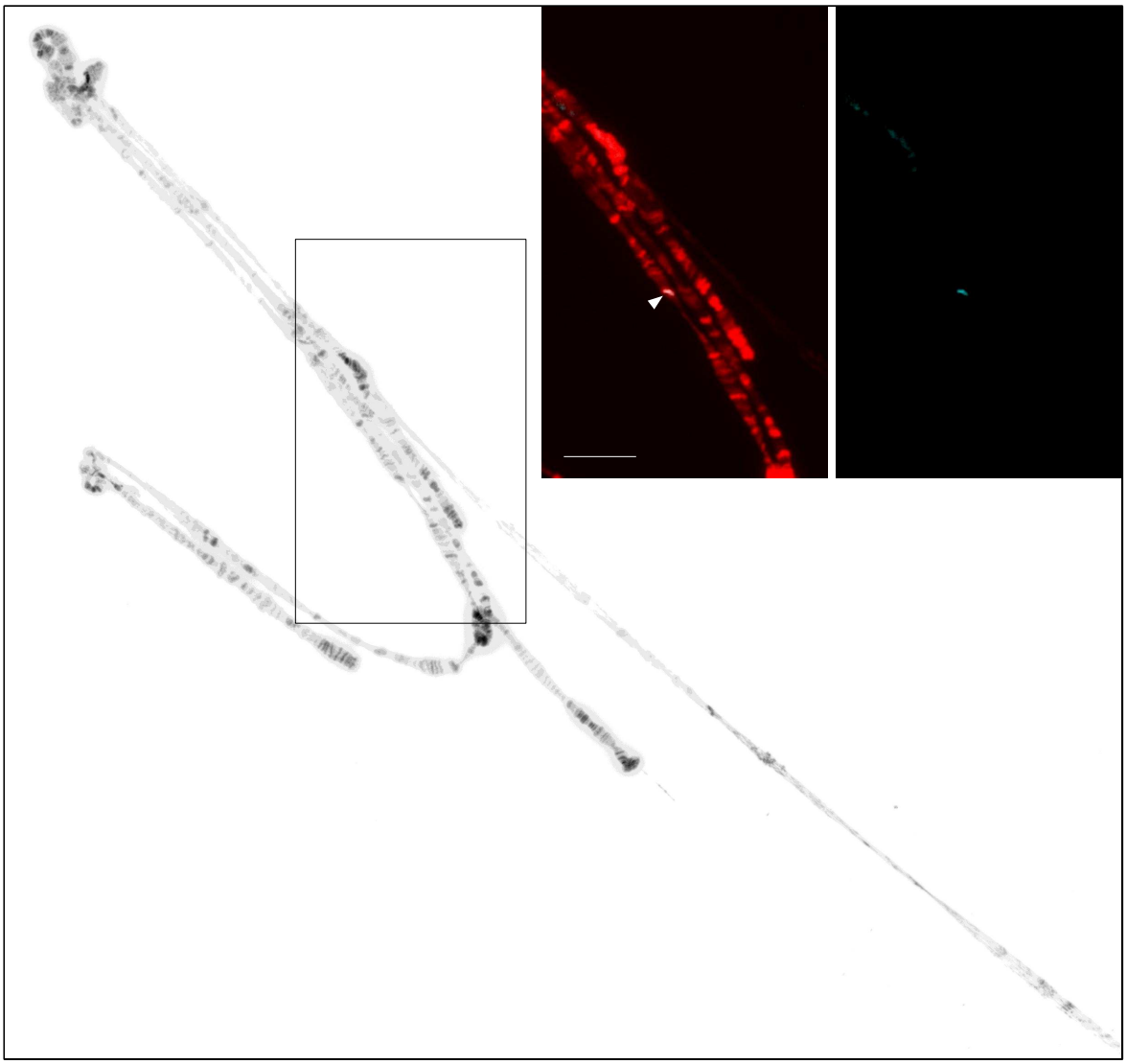

Figure S12. Localization of the *nvd* locus on *D. pachea* polytene chromosomes. A full set of polytene chromosomes is shown in inverse colors. Inset: magnification of the framed region. DNA is stained with DAPI (red) and the *nvd* locus with an Alexa488 DNA probe (magenta). The position of the *nvd* locus is indicated with a white arrowhead. Scale bar is 20 µm.

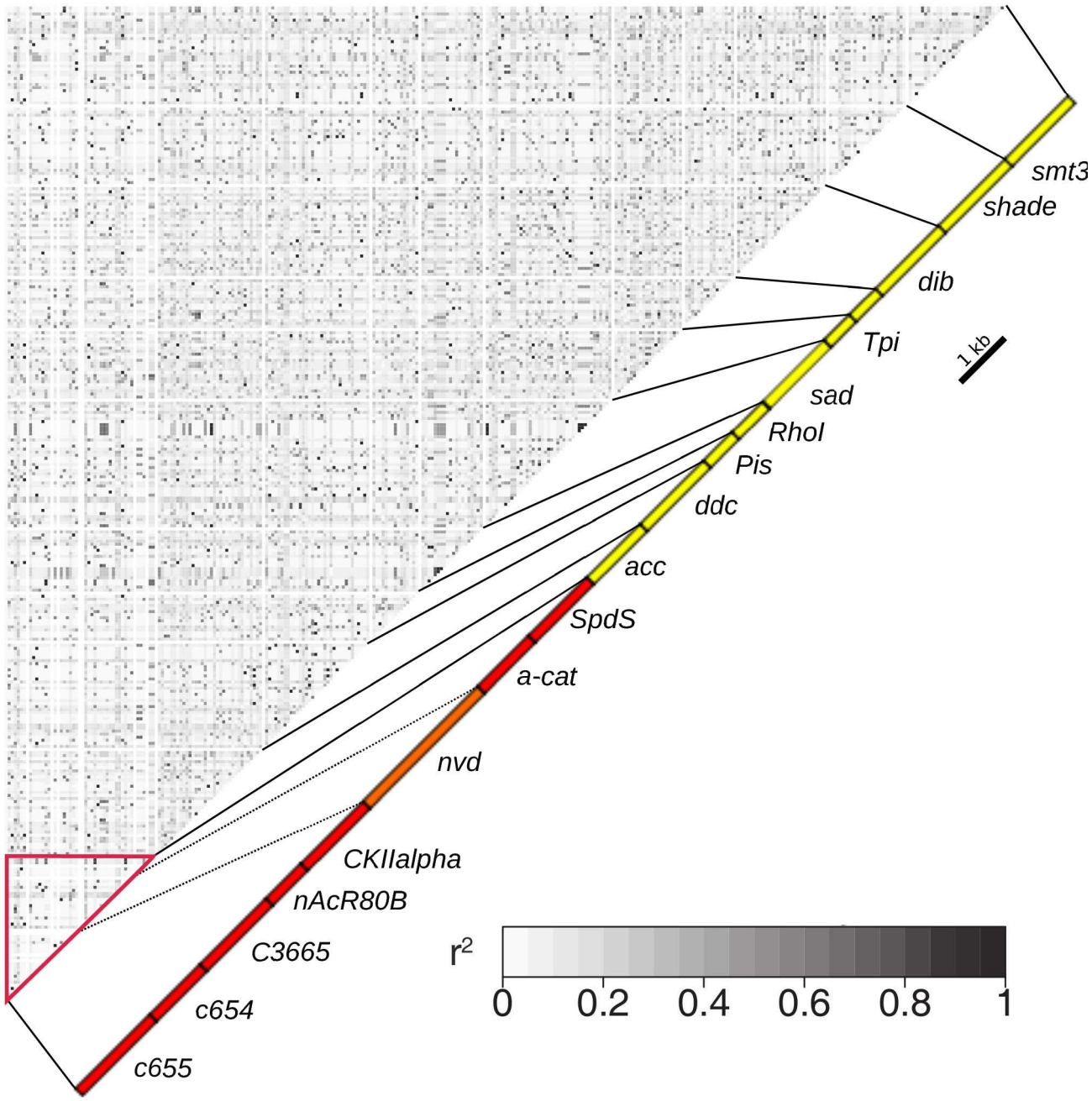

Figure S13. Linkage Disequilibrium (LD) heat map of the 272 polymorphic sites identified in 8 loci in the *nvd* region and in 9 control loci for 34 individuals. No block of nucleotides in high LD is detected in the *nvd* region (red line triangle). The *nvd* region displays a low background level of LD with a few sites in high LD, suggesting that the *nvd* region is recovering from one or several selective sweeps.

Supporting Tables

Table S1. PCR primers used in this study. See fig. S1 and Materials and Methods for details. A: PCR amplification, S: sequencing, SM: site-directed mutagenesis, F: probe synthesis for Fluorescent in situ hybridization of polytene chromosomes.

primer name	primer sequence	Used for
Nvd.ex2.F1	CCICCITWYCCNAAYGGNTGGTA	A, S
Nvd.ex2.R1	CCANTGRTGRAANGGRCATTC	A, S
Nvd.ex2.R2	CCANTGRTGRAANGGRCACTC	A, S
Nvd.ex3.F1	CCIGCIACIAARRTNAARAARTGG	A, S
Nvd.ex3.R1	TCIGGDATYTCYTGDATRTGACA	A, S
Nvd.ex5.F1	GARCCIYTIYTNCARAAGGT	A, S
Nvd.ex5.F3	GARCCIYTIATGCARAARGT	A, S
Nvd.ex6.R2	CKRWACATYTTRTGRTTCCA	A, S
Nvd.pa.ex2FF	GGATGCGTATTGCCCGCACT	A, S
Nvd.pa.ex2RR	GGAGCCATCTTTCGGCTAGAGT	A, S
iP.ac.ex5R	TGGCGCCATCTTTCGGGTAGAGT	A, S
iP.ac.ex5F	CCACAATAGTTTCAGCGCGATATGA	A, S
iP.pa.ex5R	AATTTTACTCACCATAACCGATC	A, S
iP.pa.ex5F	TAATAGTTTCAGCGCGATATGAGT	A, S
iP.ac.ex2F	AAGGGAGGTCGAGTTATAGGAGAT	A, S
iP.ac.ex2R	TTTCGATTCCCCAGCACTAAGCTT	A, S
iP.pa.ex2R	CTTCGATTCCCCCGCTCTAAGCTT	A, S
iP.ac.pa.ex2R2	CATTTGGGTATGGAGGAGGCA	A, S
iP.pa.ex2F2	GTCCCTTTCACCACTGGAGCT	A, S
5'Nvd-acR3	GCACCCAAGTGCGGGCAATATGCATCC	A, S
5robF	GCTCCCAAGTGTGGGCAATATGCATCC	A, S
3nanF	GGATGCATACTGCCCGCACTTGGGTGCT	A, S
3robF	GGATGCATATTGCCCACACTTGGGAGC	A, S
pa.finR	CCATATTTATGGCCTTCATAACA	A, S
pa.ex2F3	AAGACGATGTCAATGATAATGGA	A, S
ac.finR	GCATACGATTTACATTACTTTCA	A, S
ac.ex2F3	AGACTATGGCAATGATAAAGGA	A, S
Nvd.up2	TAATAATATGGCGAGCTACAGTTT	A, S

Nvd.do2	AATATTGGTTGCTTCAGAATATAT	A, S
pa-debut	GGAATTCATAATGGATCTGCCAACTAG	A, S
pa-stop	GGGGTACCTTACCAATCATGATTATTGGCA	A, S
ac-debut	CTCGAGTATAATGGATCTGACAACTAC	A, S
ac-stop	TCTAGATTACCAATCATGATTATTGGCA	A, S
moj-debut	GAAGATCTCACAGATGCTAACTCTACACT	A, S
moj-stop	GCTCTAGACTACCAATCTTGGCTATTTGC	A, S
5'Nvd-mojR	CCACCCGTTCGGGTAAGGCGGAGGTA	A, S
pa-nvd349F	CTTTCAAGTATCCTCTCCGAGC	A, S
pa-nvd1147R	CATCCATTTGGGTATGGAGGAG	A, S
pa-nvd1013F	GTACAAGGATCAGTGGGAAGAC	A, S
pa-nvd1997R	GACACAATAGACAGGGCTCAAC	A, S
pa-nvd1831F	GGGCAATGTTGGGAAGTGTA	A, S
pa-nvd2978R	CTCCGGTACTGTTTATGGTTCC	A, S
pa-nvd2706F	CAGATTGGACCATCCTATGTGC	A, S
pa-nvd3485R	GGGTGTGATACGACTCATTCTG	A, S
ac-nvd349F	CTTTCAAGTATGCTCTCCGTGC	A, S
ac-nvd2706F	CAGATTGGACCAGCCTATGTGC	A, S
ac-seqR	GTTGGGTTGAAAGTGGGTGTT	A, S
na-1025F	GTGGGAAGACTATGGCAGTGA	A, S
na-1920R	TACGCACCCTTCTGTGTAAC	A, S
na-nvd1790F	TGGCCACTTTCAAGCCATTCA	A, S
na-nvd2706F	CAGATTGGACCATCCTACGTAC	A, S
na-nvd321F	CGGTTCATGTCTATCGATCCA	A, S
wa-nvd1190R	CGATTCCCCCGCTCTAAGCTT	A, S
wa-nvd1013F	GTACAAGGATCAATGGGGAGAT	A, S
wa-nvd1920R	CGTGTATACCATTAGCTCTACGA	A, S
wa-nvd1771F	CGGAAAACGGCGCAGATCT	A, S
was-nvd3300R	TATGGCATTTGCACTACTTTCA	A, S
rob300F	CCGTTCATGTGAATGAACGCGA	A, S
rob1000R	TTCGCCAGCCTTAAGCGTCGA	A, S
rob3000R	AGCGAGGATTCTTCAAGTACCAG	A, S
mojG250A	tcaagagataccggaaaatgCagctgacctggcac	SM
mojP290C	ggcaggcaagttggagcTGCtcggaagccaagcacat	SM
mojL330I	ggacccgcatacgttcatAtcactttgcactcacc	SM
mojG376T	aagattactgccttaatgaagtttctaatatttACggaaactgtgatgttcg	SM
mojE377G	aagtttctaatatttggggGaactgtgatgttcgagcgg	SM
paA250G	aataccggagaacgGcgcagatctaggcc	SM
paTG376AE	atggctccaataacgaaatttttcgtatttgcggaatcggttatgtttcag	SM
paI330L	cagattggaccatcctatgtgcatctcattttgaaatcaccaa	SM
paC290R	tcataaatggactgcaagttggaatCgcaccgatcttag	SM

aCatgendebF	GAAATTCGCACCATGTCTGTAGAA	A
aCatmidR	CGTCTAATTTCACGTACTCCATCGTAA	A
aCatseqR1	AATAAAATCATTCTCGTCAACAT	A, S, F
aCatseqF4	TGTGATGCAGTCAATACTATTAG	A, S
aCatseqF5	GACATTACAACCATTGATGACTT	S, F
C3665F1	CGTCAGACAATGGAAAAGTTACATGAATAT	A, F
C3665R1	GGACGCCATTATCAGTGTTATAGTCTTCAT	A, S, F
C3665seqR2	CCCATATTTAATTTACATCTATCTGAA	A, F
C952_654F1	TTCCCAAGTCCTATTAACTGATCCTTGT	A
C952_654R1	GCGTGGATGCTTACTGCTCAT	A
C952_654SeqF1	GAATTATGAAGAAGCTGAATACTT	S
C952_655F1	AATGCGATGACAGCGTAACTGAA	A, S
C952_655R1	TTGTCGACCAATAAGCACCTTGAAT	A, S
CG12950F1	ATGCTGTAATGCTAAGAATGCCTGAA	A, S, F
CG12950R2	ACTCTGCCGGATTGACCTTGT	A, S, F
CKIIalphaF1	GCGTTTTAACTGCGTGATCTGA	A, S, F
CKIIalphaR1	AACCGTGCTGAATCGACATCTAA	A, S, F
nACRa80BF1	TGCAGGTTACTCTCTCAATCTCAATTCT	A, S
nACRa80BR1	TAAGGACGACAATCAACTGCAGAATAA	A, S
Nvd_deb	TACAAGTTTCGATTACACTTTCAAGTAT	A
nvdgenstop	CGTGACATGCTATTTAATTATTCAAT	A
NVDFL	ACTCTGACGGACGGGCGGACAC	S
SpdSF1	AATTATGGCCGGGACAATCATT	S
SpdSF2	TTGACAACGTACAAATAGAATTGAACTCTT	A
SpdSR1	CGGCATGGATTTCACTTGTGTAGTAT	A
SpdSSeqR2	GAACACTTTAATAGATACGTAAGTA	S
ACC-F	TGGTCACGCCTGAGGATCTGAA	A, F
ACC-R	CCGAACTGCGAGTCAGCAAACT	A, S, F
ACCseqF1	CTGTGCGATTCTCAAGTCAA	S
DdcF	ATGCGACGGCTCGAATCGCAAT	A
DdcR	AGACGGCCATGCGCAAGAAGT	A, S
DdcseqR2	TGGCCGTGCCTTGAATGA	S
DibF	TTGTAATTCGAGGCAATGCACGTT	A, S
DibR	CGTTCGACCACGCCAGATGA	A
DibseqF2	TCCTTGATTTCCAGCTACATT	S
PisF	GGCCATAGCCGAGCACGATAA	A, S
PisR	CTCCCTTTCGCCTTATTTCTATTCCAATT	A
PisseqR1	ACAGAGATCAGAGCCTTCA	S
Rho1F	ATGACGACGATTCGCAAGAAATTGGTAA	A
Rho1R	AGCCCTAGTTGCTGTCTCGAA	A, S
Rho1seqR2	AGGCCAACTCCACCTATAAT	S

Rho1seqF2	CTTGTGTTTGGATAATGCTTACAT	S
SadF	GTGCCAATTCCACGCGTCAA	A, S
SadR	AGGGCCAGTCGTAAGGTCTGATC	A
SadseqR1	CCACGGACCTTTCGTTCA	S
ShadeF	GTCCAATGGTAATGGCCGTCATA	A
ShadeR	CGTTTCCAGCGGTTTCACGAA	A, S
ShadeseqR2	GCCGCTATGAAGTCAATTAT	S
Smt3F	CCGTAGCTGTGAAACAATCGTGAAT	A
Smt3R	AGCCCTACGCAGAGTTGCAT	A, S
Smt3seqF2	CAAGTTGTGCGATTTCGTT	S
Smt3seqF3	CTTCGATACTAAAGTGGAGATAA	S
TpiF	GATATGTGGCATTACTTAGAGCTCCATG	A, S
TpiR	GTTCACGATGTCGACGAACTCT	A, S
TpiseqR2	GGCTTGCCATGTTTCTGA	S
TpiSeqF2	CCATACACAACCTCATCAATAT	S
Acc_A1F1	AGCTGTCAGTTGTAAGAGCGAAA	F
Acc_A1R1	CGCTCGTTCGTTCTTGAACAT	A, F
Acc_A2F1	CTGACTCGCAGTTCGGACATT	A, F
Acc_A2R1	CGAATGCTCTGCACGATTGA	A, F
Acc_A3F1	GTACGAGCTGCGTCACAATCAA	A, F
Acc_A3R1	ACGCTCTCCAATTAAGCCTCAATTA	A, F
Acc_A4F1	AGGAGGTGAAAGCTATGTTCAGGATA	A, F
Acc_A4R1	GAAATGATGGCGTCTCTTCGTA	A, F

Table S2. Annotations of *nvd* sequences from various insect species. Note that *D. virilis* genes 1 and 2 share exons 1, 2 and 3. The *D. yakuba* genome assembly (12-AUG-2009) contains a translocation within the *nvd* locus.

Species	Genome assembly	scaffold/accession number	position of first coding nucleotide	position of last coding nucleotide	orientation
Aedes aegypti	31-JAN-2009	NW_001811298/supercont1.551	198965	201009	forward
Anopheles gambiae	22-APR-2009	chromosome X/CM000360.1	unknown	19963922	reverse
Apis mellifera	27-JUL-2006	NW_001253669/Amel_4.0 GroupUn.476	unknown	15463	reverse
Bombyx mori	-	NM_001044161.1	-	-	-
Caenorhabditis elegans	-	NM_073228	-	-	-
Culex pipiens	01-DEC-2009	NW_001886820/supercont3.120	639128	631341	reverse
Drosophila ananassae	31-JUL-2008	NW_001939302/scaffold_13082	unknown	3003627	reverse
Drosophila erecta	02-AUG-2008	NW_001956549/scaffold_4784	23612898	23657602	forward
Drosophila grimshawi	17-SEP-2008	NW_001961684/scaffold_15116	744437	738868	reverse
Drosophila melanogaster	-	NM_001104200.2	-	-	-
Drosophila mojavensis	03-AUG-2008	NW_001979112/scaffold_6540	4131970	4129862	reverse
Drosophila persimilis	17-SEP-2008	NW_001985956/scaffold_3	unknown	932498	forward
Drosophila pseudoobscura	11-SEP-2008	NW_001589869/Unknown_group_7	unknown	123764	forward
Drosophila sechellia	22-APR-2009	NW_001999694/scaffold_5	141512	108741	reverse
Drosophila simulans	06-AUG-2008	NW_002044460/chr3h_Mrandom_013	83021	119107	forward
Drosophila virilis (gene 1)	04-AUG-2008	NW_002014449/scaffold_12958	2296970	2416466	forward
Drosophila virilis (gene 2)	04-AUG-2008	NW_002014449/scaffold_12958	2296970	2368098	forward
Drosophila willistoni	17-SEP-2008	NW_002032853/scf2_1100000004902	6054308	6056387	forward
Nasonia vitripennis	12-SEP-2007	NW_001819348/SCAFFOLD52	303605	308332	forward
Nasonia vitripennis	12-SEP-2007	NW_001819903/SCAFFOLD57	unknown	812375	reverse
Spodoptera littoralis	01-FEB-2011	GU391576	-	-	-

Table S3. PAML analyses of the *nvd* coding sequences across the Diptera phylogeny. We tested a branch model, where the null model is a single ω (dN/dS) ratio over the entire tree and the alternative model is two ω values, one for the *D. pachea* lineage and one for the rest of the tree. Analyses were done either with the inclusion or the exclusion of the mosquitoes sequences, because of possible saturation of dS to these lineages. Both analyses indicate that ω_{pachea} is significantly higher than for the rest of the tree. This suggests that either positive selection or relaxed purifying selection occurred in *nvd* in this lineage.The free ratio model was used to estimate ω on each branch (fig. S2).

			Ln(L)
Drosophila and mosquitoes	free ratios model	$\omega_{pachea} = 0.231$	-10637.1983
Drosophila and mosquitoes	Ho : one ratio, $\omega_{pachea} = \omega_{others}$	$\omega = 0.120$	-10676.1950
Drosophila and mosquitoes	H1 : two ratios, $\omega_{pachea} \neq \omega_{others}$	$\omega_{pachea} = 0.261$ $\omega_{others} = 0.118$	-10673.4820
Ho v H1 : df = 1	LRT = 2 (lnL1-lnL2) = 5.4259	$p < 0.0199$	significant
Drosophila only	Ho : one ratio, $\omega_{pachea} = \omega_{others}$	$\omega = 0.123$	-8269.7651
Drosophila only	H1 : two ratios, $\omega_{pachea} \neq \omega_{others}$	$\omega_{pachea} = 0.260$ $\omega_{others} = 0.120$	-8267.1138
Ho v H1 : df = 1	LRT = 2 (lnL1-lnL2) = 5.3026	$p < 0.0214$	significant

Table S4. Progeny number of the rescue experiments of *D. melanogaster nvd* RNAi flies.

The number of adult progeny flies from two crosses is shown. Cross 1: *D. melanogaster* females *UAS-nvd-RNAi/CyO* x males *UAS-nvd-pa/Y; 2-286-GAL4/TM3 Sb.* Cross 2: *D. melanogaster* females *UAS-nvd-RNAi/CyO* x males *UAS-nvd-pa-4mut/Y; 2-286-GAL4/TM3 Sb.* Only tubes where the total number of progeny exceeded 50 were considered for the statistical analysis (see main paper) and for Fig. 2.

Cross 1

Total number of flies	Relative proportion of *2-286-GAL4*	Relative proportion of *2-286>nvdRNAi*	Relative proportion of *2-286>nvdRNAi, nvd-pa*	Number of *Sb* males (reference genotype)	Number of *2-286-GAL4*	Number of *2-286>nvdRNAi*	Number of *2-286>nvdRNAi, nvd-pa*
normal food							
131	100,00	0,00	0,00	20	20	0	0
107	128,57	0,00	0,00	14	18	0	0
138	217,65	0,00	0,00	17	37	0	0
102	108,33	0,00	0,00	12	13	0	0
160	67,74	0,00	0,00	31	21	0	0
7	50,00	0,00	0,00	2	1	0	0
123	81,82	0,00	4,55	22	18	0	1
134	57,69	0,00	3,85	26	15	0	1
192	120,83	0,00	0,00	24	29	0	0
10	133,33	0,00	0,00	3	4	0	0
15	33,33	0,00	0,00	6	2	0	0
127	41,67	0,00	0,00	24	10	0	0
82	57,14	0,00	0,00	14	8	0	0
63	142,86	0,00	0,00	7	10	0	0
44	62,50	0,00	0,00	8	5	0	0
68	110,00	0,00	0,00	10	11	0	0
95	120,00	0,00	0,00	15	18	0	0
101	84,62	0,00	0,00	13	11	0	0
89	106,67	0,00	0,00	15	16	0	0
58	112,50	0,00	0,00	8	9	0	0
70	61,11	0,00	0,00	18	11	0	0
normal food + 7DHC							
43	140,00	120,00	100,00	5	7	6	5
29	300,00	300,00	700,00	1	3	3	7
59	54,55	36,36	63,64	11	6	4	7
128	116,67	116,67	183,33	12	14	14	22
84	155,56	77,78	88,89	9	14	7	8
21	100,00	100,00	250,00	2	2	2	5
82	50,00	100,00	75,00	12	6	12	9
8	25,00	0,00	50,00	4	1	0	2
168	81,82	113,64	131,82	22	18	25	29
109	140,00	130,00	200,00	10	14	13	20
134	66,67	109,52	109,52	21	14	23	23
163	82,14	67,86	75,00	28	23	19	21
142	73,91	86,96	91,30	23	17	20	21
79	122,22	133,33	55,56	9	11	12	5
126	105,88	111,76	105,88	17	18	19	18
normal food + lathosterol							
127	170,00	0,00	340,00	10	17	0	34
188	106,67	0,00	150,00	30	32	0	45
153	105,56	0,00	122,22	18	19	0	22
69	72,73	0,00	109,09	11	8	0	12
40	350,00	0,00	550,00	2	7	0	11
97	108,33	0,00	191,67	12	13	0	23
168	63,64	0,00	115,15	33	21	0	38
212	63,41	0,00	70,73	41	26	0	29
125	110,00	0,00	300,00	10	11	0	30
95	127,27	0,00	154,55	11	14	0	17
81	57,14	7,14	128,57	14	8	1	18

Cross 2

Total number of flies	Relative proportion of *2-286-GAL4*	Relative proportion of *2-286>nvdRNAi*	Relative proportion of *2-286>nvdRNAi, nvd-pa-4-mut*	Number of *Sb* males (reference genotype)	Number of *2-286-GAL4*	Number of *2-286>nvdRNAi*	Number of *2-286>nvdRNAi, nvd-pa-4-mut*
normal food							
170	118.18	0.00	118.18	22	26	0	26
35	180.00	0.00	80.00	5	9	0	4
67	112.50	0.00	75.00	8	9	0	6
72	33.33	0.00	60.00	15	5	0	9
45	120.00	0.00	40.00	5	6	0	2
158	113.04	0.00	82.61	23	26	0	19
150	157.14	0.00	121.43	14	22	0	17
81	56.25	0.00	68.75	16	9	0	11
101	180.00	0.00	150.00	10	18	0	15
90	76.47	0.00	82.35	17	13	0	14
102	78.57	0.00	121.43	14	11	0	17
138	61.11	0.00	105.56	18	11	0	19
normal food + 7DHC							
293	87.80	92.68	87.80	41	36	38	36
204	90.91	104.55	122.73	22	20	23	27
116	366.67	277.78	44.44	9	33	25	4
77	41.67	83.33	91.67	12	5	10	11
192	71.43	82.14	96.43	28	20	23	27
163	105.56	166.67	138.89	18	19	30	25
193	64.00	120.00	88.00	25	16	30	22
normal food + lathosterol							
72	130.00	0.00	120.00	10	13	0	12
81	64.71	0.00	47.06	17	11	0	8
102	78.95	0.00	73.68	19	15	0	14
194	91.43	0.00	102.86	35	32	0	36
291	118.60	2.33	106.98	43	51	1	46
130	71.43	0.00	133.33	21	15	0	28
68	40.00	0.00	140.00	10	4	0	14
66	41.67	0.00	116.67	12	5	0	14
137	80.77	0.00	100.00	26	21	0	26
42	54.55	0.00	109.09	11	6	0	12

Table S5. Sex of the 34 individuals used for population genetics analysis.

Individual name	Alternative name	Bottle from which it was collected	Sex
1_1	1	1	male
1_2	2	1	male
1_3	3	1	male
1_4	4	1	male
1_5	5	1	female
1_7	7	1	female
1_8	8	1	female
1_9	9	1	female
1_10	10	1	female
1_11	11	1	female
1_12	12	1	female
1_13	13	1	female
1_14	14	1	female
2_1	15	2	male
2_2	16	2	female
2_3	17	2	male
2_4	18	2	male
2_5	19	2	male
2_6	20	2	female
2_7	21	2	female
2_8	22	2	female
2_9	23	2	female
2_10	24	2	female
2_11	25	2	female
2_12	26	2	female
2_13	27	2	female
2_14	28	2	female
2_15	29	2	female
2_16	30	2	male
2_17	31	2	female
2_18	32	2	female
2_19	33	2	female
2_20	34	2	female
2_21	35	2	female

Table S6. Polymorphism statistics of the sequences obtained from the 34 *D. pachea* individuals. There is a 10 fold difference in nucleotide diversity between the eight genes that are within the *nvd* scaffold and the nine control genes. All three of the simple tests of selection (Tajima's D, and the two Fu and Li tests) show that there is evidence for purifying selection and/or recovery from a selective sweep in the *nvd* region and not across the control regions. The column headings are: Nchrom: number of chromosomes in the test (34 individuals yielded 68 phased haplotypes for autosomal genes and 59 phased haplotypes for sex-linked genes). Seg. Sites: number of segregating sites; TotSites: total number of sites sequenced; rho: estimate of rho = 4NR per site. NA: not applicable. References for nucleotide diversity (π), Watterson's theta or mutation rate (θw), Tajima's D, Fu and Li D*, Fu and Li F*, Zns and rho statistics can be found in (*39*). Values in grey background are significant ($p < 0.05$).

Gene	Nchroms	Seg. Sites	TotSites	π + SD	θw	Tajima_D	FuLi_D*	FuLi_F*	ZnS	rho
C952	68	7	1733	0.00034 + 0.00006	0.00084	-1.48866	-2.07172	-2.21526	0.0568	0.0390
C952-654	68	7	1235	0.00026 + 0.00007	0.00118	-1.95324	-2.07172	-2.39493	0.0005	0.0390
C3665	68	1	1565	0.00002 + 0.00002	0.00013	-1.07049	-1.92845	-1.94484	NA	NA
nACR80B	68	6	874	0.00048 + 0.00012	0.00143	-1.5953	-0.6593	-1.13221	0.0187	0.0252
CKIIalpha	68	0	1489	0	0.00000	0	0	0	NA	NA
nvd	68	16	2669	0.00071 + 0.00009	0.00124	-1.27579	-1.71606	-1.85416	0.0483	0.0021
acat	68	3	1247	0.00007 + 0.00005	0.00050	-1.66053	-3.20311	-3.18649	0.3335	0
SpdS	68	2	1384	0.00016 + 0.00007	0.00030	-0.76772	0.71782	0.31425	1.0000	0
acc	68	34	1295	0.00427 + 0.00024	0.00564	-0.78703	0.63404	0.11975	0.0300	0.1229
ddc	68	34	1522	0.00246 + 0.00018	0.00466	-1.52499	-2.63026	-2.64712	0.0434	0.0406
Pis	68	15	731	0.00257 + 0.00027	0.00457	-1.29247	-1.24062	-1.49579	0.0360	0.1411
Rhol	68	20	777	0.00324 + 0.00038	0.00564	-1.30812	-0.21446	-0.72619	0.0698	0.0142
sad	68	41	1511	0.00339 + 0.00025	0.00594	-1.41375	-1.96955	-2.10248	0.0443	0.1577
Tpi	68	16	657	0.00349 + 0.00180	0.00508	-0.92787	-0.76517	-0.97747	0.0411	0.1460
dib	59	29	1519	0.00339 + 0.00014	0.00399	-0.47396	-0.5651	-0.63414	0.0414	0.1825
shade	59	25	1600	0.00175 + 0.00015	0.00339	-1.51971	-0.82612	-1.28946	0.0359	0.0832
smt3	59	32	1482	0.00287 + 0.00019	0.00465	-1.23058	-1.65215	-1.78496	0.0427	0.0636

Table S7. Table contrasting the population genetics attributes of the *nvd* region compared to control loci. The population recombination rate in the *nvd* region is low (grey background) compared to the control loci. These data are consistent with the presence of only 4 recombination events in the *nvd* region across this sample, as compared to 53 recombination events in the control genes. Note that for the purpose of this analysis, the sequences of the *nvd* region were concatenated according to their order and orientation along the *nvd* scaffold. Those of the control loci were also concatenated. Since the 9 control loci probably lie relatively far from each other in the genome, it means that there are probably 53 -9 +1 = 45 recombination events within the 9 loci.

	***nvd* region**	**control loci**
Size of the region	12 212	11 763
Number of segregating sites	42	268
Nucleotide diversity (π)	0.00029	0.0031
θs	0.00072	0.0049
Tajima's D	-1.945	-1.283
Fu and Li D*	-2.734	-1.286
Fu and Li F*	-2.911	-1.541
Zns	0.0346	0.0203
rho = 4Nr	0.0018	0.0547
Inferred number of recombination events	4	53

Table S8. Table of synonymous and non synonymous divergence between *D. pachea* and *D. mojavensis*. Nsites: total number of sites analyzed in the coding regions, SynDiffs: count of synonymous differences, SynPosns: synonymous positions, Ks: rate of substitution per synonymous site, NsynDiffs: count of nonsynonymous differences, NsynPosns: count of nonsynonymous positions, Ka: rate of nonsynonymous substitution per nonsynonymous site, NA: not applicable. Note that all the genes look like typical conserved coding regions, with most nonsynonymous changes having been removed by purifying natural selection. *nvd* has a rather high Ka, but *C952* is a bit higher (but the Ka/Ks ratio is highest for *nvd*). This alone does not suggest selection, but this is perhaps not expected, since it only took 4 amino acid changes to lose cholesterol conversion. Note also that Ks are significantly higher for the *nvd* region than for the control genes (two-sided t-test, $p < 0.0031$), whereas Ka values are similar (two-sided t-test, $p > 0.18$).

Gene name	Nsites	SynDiffs	SynPosns	Ks	NsynDiffs	NsynPosns	Ka	Ka/Ks
***nvd* region**								
C952	1746	263.58	369.58	2.2607	324.42	1355.42	0.2883	0.1275
C952-654	966	131.17	214.83	1.2618	70.83	751.17	0.1008	0.0799
C3665	798	133.17	195.67	1.7849	25.83	599.33	0.0444	0.0249
nACR80B	573	81.5	137.42	1.1733	9.5	435.58	0.0221	0.0188
CKIIalpha	1008	109	225.25	0.7772	2	782.75	0.0026	0.0033
nvd	1113	167.83	244.5	1.851	183.17	871.5	0.2466	0.1332
acat	974	136	226	1.216	16	746	0.0218	0.0179
SpdS	807	116.5	175.58	1.62	50.5	631.42	0.0846	0.0522
autosomal loci								
acc	959	122	234.5	0.8873	2	722.5	0.0028	0.0032
ddc	1215	152.5	288.25	0.9166	23.5	926.75	0.0258	0.0281
Pis	132	19	32.58	1.1271	2	99.42	0.0204	0.0181
Rhol	312	10	69.83	0.1589	3	242.17	0.0125	0.0787
sad	1200	150.08	290.42	0.8761	94.92	909.58	0.1124	0.1283
Tpi	594	56.83	144.92	0.555	26.17	449.08	0.0607	0.1094
X-linked loci								
dib	1302	189.25	332.25	1.0687	87.75	969.75	0.0964	0.0902
shade	1227	121.5	302.42	0.5754	20.5	924.58	0.0225	0.0391
smt3	60	14	13.5	NA	0	46.5	0	NA

Table S9. Table of MacDonald-Kreitman scores in *D. pachea*. Ncodons: number of codons, SynPoly: number of synonymous polymorphic sites within *D. pachea*, SynDifs: number of fixed synonymous differences between *D. pachea* and *D. mojavensis*, NsynPoly: number of nonsynonymous polymorphic sites within *D. pachea*, NsynDifs: number of fixed nonsynonymous differences between *D. pachea* and *D. mojavensis*. The genes in the *nvd* region have low levels of polymorphism (see also Table S4) and only *NAcR80B* attains nominal significance, but this is not significant after correcting for the fact that 17 tests were performed. None of the control loci yield a signature of natural selection either.

Gene name	Ncodons	SynPoly	SynDifs	NsynPoly	NsynDifs	P value
***nvd* region**						
C952	251	3	137	1	60	0.7533
C952-654	322	4	135	0	64	0.4081
C3665	217	0	117	1	11	1.0000
NAcR80B	165	2	70	3	8	0.0124
CKIIalpha	336	0	109	0	2	1.0000
nvd	207	1	154	1	69	0.8513
acat	227	1	97	1	10	0.4800
SpdS	222	1	110	1	28	0.8803
autosomal loci						
acc	329	13	117	1	2	0.7260
ddc	397	13	146	4	20	0.3378
Pis	44	3	18	0	2	0.5990
Rhol	77	1	9	0	1	0.1356
sad	151	8	61	5	29	0.8952
Tpi	151	6	45	2	15	0.6638
X-linked loci						
dib	357	17	152	5	51	0.9900
shade	411	16	121	0	18	0.2631
smt3	20	1	12	0	0	1.0000
Total						
***nvd* region**	1947	12	929	8	252	0.0826
control loci	1937	78	681	17	138	0.9124

Table S10. GC content in *D. pachea* and *D. mojavensis* coding genes. The coding regions that were sequenced in the 34 *D. pachea* individuals were aligned to *D. mojavensis* sequences and we calculated the percentage of GC in the aligned regions from *D. pachea* and *D. mojavensis*. The percentage of GC is significantly different between the *nvd* region and the control loci (Wilcoxon rank test, $p < 0.0018$).

	D. pachea		***D. mojavensis***	
Gene name	**Length**	**CG%**	**Length**	**CG%**
***nvd* region**				
C952	1743	0.45	1728	0.36
C952-654	966	0.40	966	0.36
C952	1743	0.45	1728	0.36
C3665	798	0.47	795	0.42
nAcR80B	573	0.42	573	0.42
CKIIalpha	1008	0.44	1008	0.42
nvd	1116	0.43	1308	0.37
acat	974	0.46	1095	0.41
SpdS	807	0.42	744	0.36
average	**9728**	**0.44**	**9945**	**0.39**
control loci				
acc	959	0.58	959	0.58
ddc	1215	0.57	1215	0.60
dib	1307	0.57	1304	0.57
pis	133	0.47	133	0.48
RhoI	312	0.45	312	0.45
sad	1208	0.55	1202	0.55
shade	1227	0.58	1235	0.57
smt3	61	0.59	72	0.43
Tpi_1	152	0.42	149	0.42
Tpi_2	596	0.61	596	0.59
average	**7170**	**0.54**	**7177**	**0.52**

References

18. L. Timmons *et al.*, Green fluorescent protein/β-galactosidase double reporters for visualizing Drosophila gene expression patterns, *Developmental Genetics* , 338–347 (1997).

19. A. M. Huang, E. J. Rehm, G. M. Rubin, Recovery of DNA sequences flanking P-element insertions in Drosophila: inverse PCR and plasmid rescue, *Cold Spring Harb Protoc* **2009**, pdb.prot5199 (2009).

20. K. Rutherford *et al.*, Artemis: sequence visualization and annotation, *Bioinformatics* **16**, 944–945 (2000).

21. P. C. Ng, S. Henikoff, SIFT: Predicting amino acid changes that affect protein function, *Nucleic Acids Res* **31**, 3812–3814 (2003).

22. T. Hall, BioEdit: a user-friendly biological sequence alignment editor and analysis program for Windows 95/98/NT, *Nucleic Acids Symposium Series* **41**, 95–98 (1999).

23. Z. Yang, PAML 4: Phylogenetic Analysis by Maximum Likelihood, *Molecular Biology and Evolution* **24**, 1586 –1591 (2007).

24. M. Wessner *et al.*, Ecdysteroids from Ajuga iva, *Phytochemistry* **31**, 3785–3788 (1992).

25. J.-P. Girault *et al.*, Ecdysteroids from Leuzea carthamoides, *Phytochemistry* **27**, 737–741 (1988).

26. R. Niwa *et al.*, CYP306A1, a cytochrome P450 enzyme, is essential for ecdysteroid biosynthesis in the prothoracic glands of Bombyx and Drosophila, *J. Biol. Chem* **279**, 35942–35949 (2004).

27. J. T. Warren *et al.*, Molecular and biochemical characterization of two P450 enzymes in the ecdysteroidogenic pathway of Drosophila melanogaster, *Proc. Natl. Acad. Sci. U.S.A* **99**, 11043–11048 (2002).

28. G. E. Roth *et al.*, The Drosophila gene Start1: a putative cholesterol transporter and key regulator of ecdysteroid synthesis, *Proc. Natl. Acad. Sci. U.S.A* **101**, 1601–1606 (2004).

29. A. E. Christian, M. P. Haynes, M. C. Phillips, G. H. Rothblat, Use of cyclodextrins for manipulating cellular cholesterol content, *J. Lipid Res* **38**, 2264–2272 (1997).

30. S. Lavrov, J. Déjardin, G. Cavalli, Combined immunostaining and FISH analysis of polytene chromosomes, *Methods Mol. Biol.* **247**, 289–303 (2004).

31. D. R. Zerbino, E. Birney, Velvet: algorithms for de novo short read assembly using de Bruijn graphs, *Genome Res.* **18**, 821–829 (2008).

32. H. Li, R. Durbin, Fast and accurate short read alignment with Burrows-Wheeler transform, *Bioinformatics* **25**, 1754–1760 (2009).

33. J. T. Robinson *et al.*, Integrative genomics viewer, *Nature Biotechnology* **29**, 24–26 (2011).

34. A. Drummond *et al.*, *Geneious* (2011; http://www.geneious.com/).

35. D. A. Dmitriev, R. A. Rakitov, Decoding of superimposed traces produced by direct sequencing of heterozygous indels, *PLoS Comput. Biol.* **4**, e1000113 (2008).

36. M. Stephens, N. J. Smith, P. Donnelly, A new statistical method for haplotype reconstruction from population data, *Am. J. Hum. Genet.* **68**, 978–989 (2001).

37. J. K. Pritchard, M. Stephens, P. Donnelly, Inference of population structure using multilocus genotype data, *Genetics* **155**, 945–959 (2000).

38. D. Reich, A. L. Price, N. Patterson, Principal component analysis of genetic data, *Nat. Genet.* **40**, 491–492 (2008).

39. P. Librado, J. Rozas, DnaSP v5: a software for comprehensive analysis of DNA polymorphism data, *Bioinformatics* **25**, 1451–1452 (2009).

40. J. H. McDonald, M. Kreitman, Adaptive protein evolution at the Adh locus in Drosophila, *Nature* **351**, 652–654 (1991).

41. R. R. Hudson, M. Kreitman, M. Aguadé, A test of neutral molecular evolution based on nucleotide data, *Genetics* **116**, 153–159 (1987).

42. Y. Kim, R. Nielsen, Linkage disequilibrium as a signature of selective sweeps, *Genetics* **167**, 1513–1524 (2004).

43. Y. Kim, W. Stephan, Detecting a local signature of genetic hitchhiking along a recombining chromosome, *Genetics* **160**, 765–777 (2002).

44. P. Pavlidis, N. Alachiotis, OmegaPlus 2.0.0 software (2012) (available at http://sco.h-its.org/exelixis/software/OmegaPlus_Manual.pdf).

45. R. R. Hudson, Generating samples under a Wright-Fisher neutral model of genetic variation, *Bioinformatics* **18**, 337–338 (2002).

46. P. Sabeti, Sweep software (available at http://www.broadinstitute.org/mpg/sweep/index.html).

47. D.V. Zaykin, A. Pudovkin, B.S. Weir, Correlation-based inference for linkage disequilibrium with multiple alleles, *Genetics* **180**, 533–545 (2008).

48. J.-H. Shin, S. Blay, B. McNeney, J. Graham, LDheatmap: An R Function for Graphical Display of Pairwise Linkage Disequilibria Between Single Nucleotide Polymorphisms, *Journal of Statistical Software* **16** (available at http://rgm2.lab.nig.ac.jp/RGM2/func.php?rd_id=LDheatmap:LDheatmap).

49. S. Nishi, H. Nishino, T. Ishibashi, cDNA cloning of the mammalian sterol C5-desaturase and the expression in yeast mutant, *Biochim. Biophys. Acta* **1490**, 106–108 (2000).

50. G. Vinci, X. Xia, R. A. Veitia, Preservation of genes involved in sterol metabolism in cholesterol auxotrophs: facts and hypotheses, *PLoS ONE* **3**, e2883 (2008).

51. S. W. Schaeffer *et al.*, Polytene chromosomal maps of 11 Drosophila species: the order of genomic scaffolds inferred from genetic and physical maps, *Genetics* **179**, 1601–1655 (2008).

52. J. C. Yasuhara, C. H. DeCrease, B. T. Wakimoto, Evolution of heterochromatic genes of Drosophila, *Proc. Natl. Acad. Sci. U.S.A.* **102**, 10958–10963 (2005).

53. S. R. Schulze *et al.*, Heterochromatic genes in Drosophila: a comparative analysis of two genes, *Genetics* **173**, 1433–1445 (2006).

54. T. F. C. Mackay *et al.*, The Drosophila melanogaster Genetic Reference Panel, *Nature* **482**, 173–178 (2012).

55. R. J. Kulathinal, S. M. Bennett, C. L. Fitzpatrick, M. A. F. Noor, Fine-scale mapping of recombination rate in Drosophila refines its correlation to diversity and divergence, *Proc. Natl. Acad. Sci. U.S.A.* **105**, 10051–10056 (2008).

56. A. G. Clark *et al.*, Evolution of genes and genomes on the Drosophila phylogeny, *Nature* **450**, 203–218 (2007).

57. B. L. Ward, W. B. Heed, Chromosome phylogeny of *Drosophila pachea* and related species, *J. Hered.* **61**, 248-258 (1970).